

APPENDIX B
APPROXIMATE METHODS FOR ANALYSIS OF FLOW PROBLEMS

B-1. Introduction. As previously mentioned in Chapter 4, various methods are available, in addition to flow nets, for solving idealization of seepage problems. As shown in figure 4-3, these methods include electrical analogy, hydraulic or sand tank models, viscous flow models, method of fragments, finite difference method, and finite element method. Prior to conducting an analysis, the problem to be studied must be defined in terms of:

- a. Aquifer and embankment dimensions.
- b. Coefficients of permeability of the embankment and foundation soils.
- c. Horizontal to vertical permeability ratios.
- d. Boundary conditions (impermeable and symmetrical).
- e. Exits and entrances (fixed potential areas).
- f. Head versus time relationships for unsteady flow.

Sensitivity studies may be run to establish the effect of parameters not known accurately.

B-2. Electrical Analogy.

a. General. Processes which involve movement of current due to differences in energy potential operate on the same principles as movement of confined ground water as shown in table B-1. Therefore, to obtain the pattern of equipotential lines or flow lines (see figure 4-4), the flow domain is transferred by an electrical conductor of similar geometric form as first proposed by Pavlovsky in 1918 (Harr 1962). Electrical analogies may involve two-dimensional conducting paper models or three-dimensional tanks containing aqueous solution.

b. Two-Dimensional Models. When field conditions can be approximated by a two-dimensional plan or section, teledeltos conducting paper models may be used to obtain a flow net. Two-dimensional teledeltos models are simple to use and can accommodate various geometries. However, it is difficult to simulate varying permeabilities and they are generally restricted to steady state confined aquifers (Bear 1972, Boer and Molen 1972).

c. Three-Dimensional Models. The use of electrical analogy models is described by various authors (Zangar 1953, Todd and Bear 1959, and Duncan 1963). The three-dimensional electrical analogy model at the U. S. Army Engineer Waterways Experiment Station (WES) (see figure B-1) is a plexiglass tank filled with dilute copper sulfate solution and having a calibrated elevated carrier assembly for the accurate placement of a point electrode probe

30 Sep 86

Table B-1. Analogy Between Darcy's Law and Ohm's Law^(a)

Darcy's Law	Ohm's Law
$Q = \frac{KAH}{L}$	$I = \frac{K'A'V}{L'}$
Q = rate of flow or water	I = current (rate of flow of electricity)
K = coefficient of permeability	K' = conductivity coefficient
A = cross-sectional area	A' = cross-sectional area
H = head producing flow	V = voltage producing current
L = length of path of percolation	L' = length of path of current

(a) From Bureau of Reclamation. ¹²⁷

anywhere in the fluid. Extensive use of the WES model has been made to:

(1) Determine uplift values and seepage quantities for use in the design of Columbia Lock and Dam, Louisiana (Duncan 1962).

(2) Determine the uplift values and seepage quantities for fully and partially penetrating well arrays from line and circular sources (Duncan 1963, Banks 1963, and Banks 1965).

(3) Determine uplift pressures beneath the spillway, piezometric heads at the downstream toe of the dam, and total seepage quantities for use in the design of Oakley Dam, Illinois (McAnear and Trahan 1972).

B-3. Sand Tank Model. The sand tank model (hydraulic model), as shown in figure B-2, consists of a rigid, watertight container with a transparent front, filled with sand, deaired water,⁽¹⁾ and measuring devices. The geometry of the sand tank corresponds to that of the prototype. The sand may be placed under water to provide a homogeneous condition, or layers of different sand sizes may be used to study anisotropy. If the flow is unconfined and the same material is used for model and prototype, the capillary rise must be compensated for in the model. When a steady-state flow is reached, dye can be introduced at various points along the upstream boundary close to the front wall to form traces of the streamlines. Piezometers are used to measure the pressure heads at various locations (Bear 1972 and Harr 1962). A sand tank model was employed to investigate the effect of length of horizontal drain on the through seepage flow nets and quantities for a homogeneous and isotropic sand embankment

⁽¹⁾ For prolonged tests, disinfectants such as Formol should be added to the water to prevent bacterial growth that causes clogging (Bear 1972).

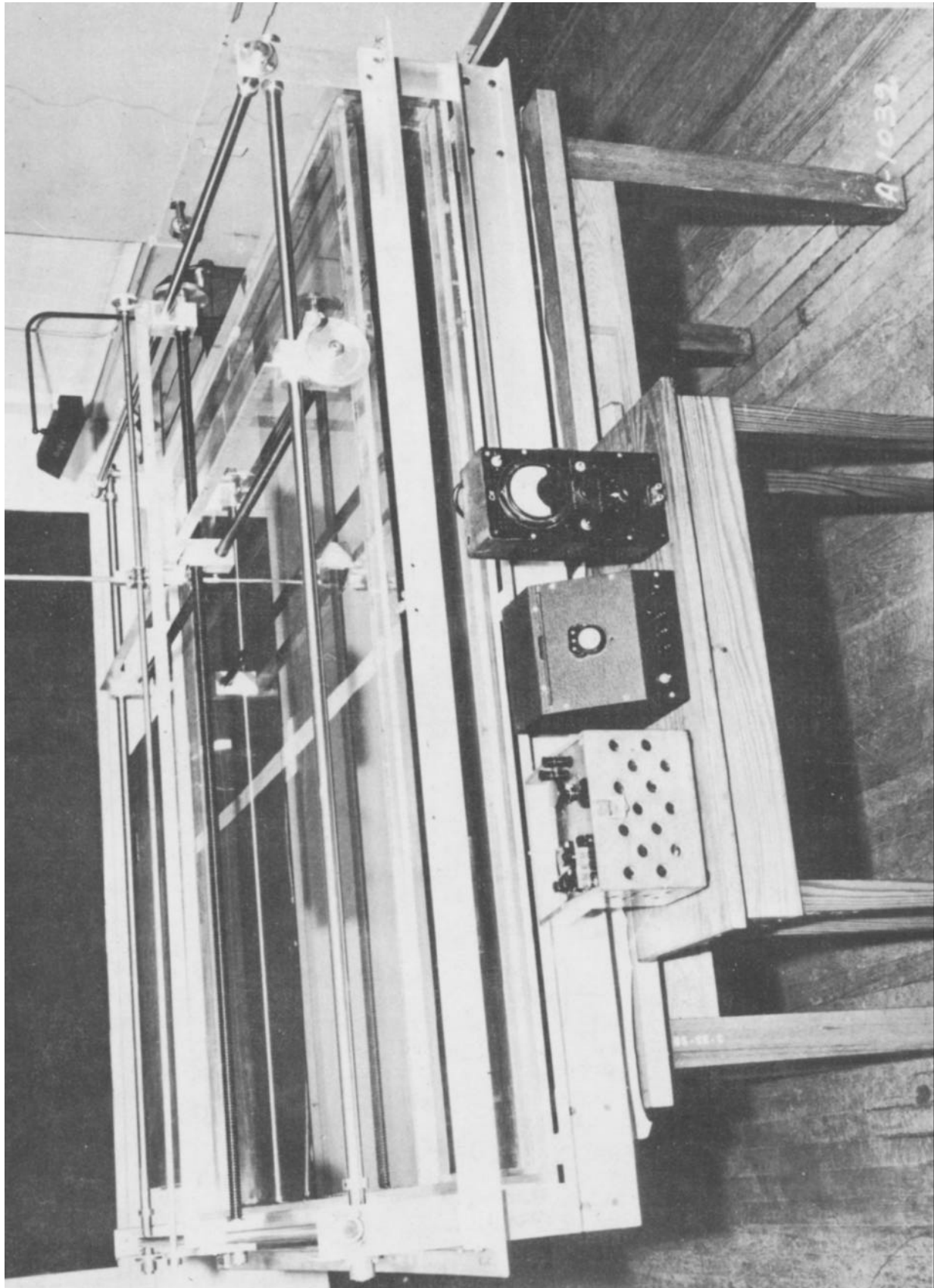
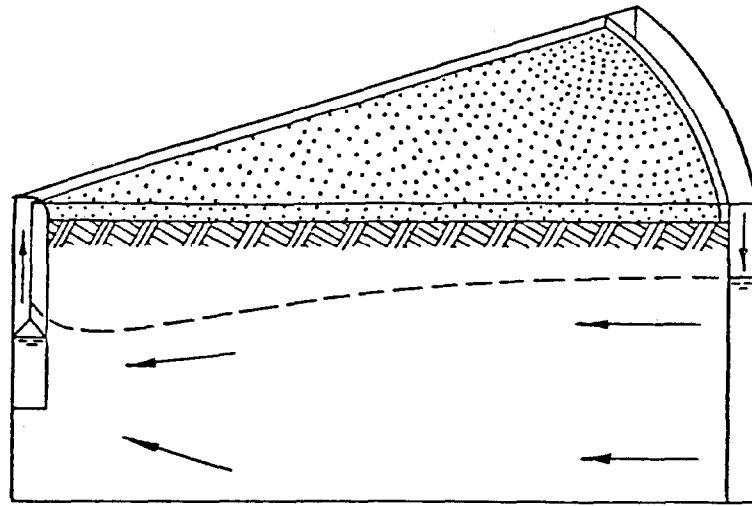
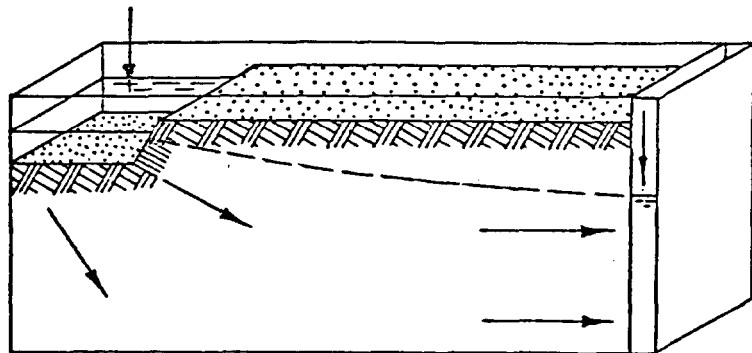


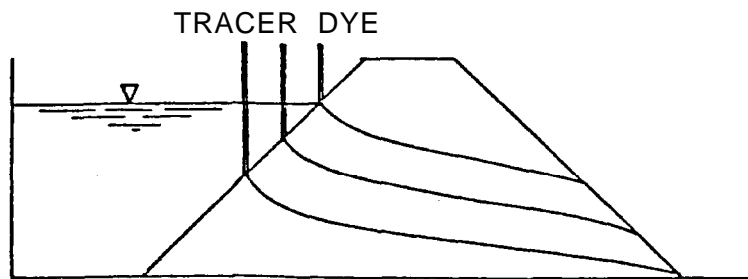
Figure B-1. Three-dimensional electrical analogy apparatus (after Duncan³⁶)



PARTIALLY PENETRATING WELL
WITH A CIRCULAR SOURCE



SEEPAGE FROM CANALS



SEEPAGE IN EMBANKMENTS

Figure B-2. Hydraulic or sand tank model
(prepared by WES)

(Brand and Armstrong 1968). Sand tank models are also used extensively in petroleum engineering, ground-water quality, and pollution research (Bear 1972 and Prickett 1979).

B-4. Viscous Flow Models. The viscous flow model, also called the Hele-Shaw or parallel plate model, is based on the similarity between the differential equations governing saturated flow in a porous medium and those describing the flow of a viscous liquid in the narrow space between two parallel plates. The viscous flow model contains the shape of the structure to be investigated and once a steady-state flow is obtained, colored dyes can be injected along the upstream edge and patterns of streamlines can be observed. A camera (movie or still) is normally used to record the results of experiments. Inhomogeneous hydraulic conductivity, such as would exist in a zoned earth dam, can be simulated by varying the width of the interspace between the parallel plates, as shown in figure B-3. The viscous flow model experiments should be conducted in a temperature-controlled room because viscosity plays an important role in analog scaling. If this is not feasible, the temperature should be measured at all inflow and outflow points during the test and scales must be recomputed according to the varying average temperature of the liquid in the model (Bear 1972 and Harr 1962). A viscous flow model was constructed at WES to simulate seepage conditions induced in streambanks by sudden drawdown of the river level. The results from the model study compared favorably with field observations, finite difference, and finite element methods (Desai 1970 and Desai 1973).

B-5. Method of Fragments.

a. General. The method of fragments is an approximate analytical method for the computation of flows and pressure heads for any ground-water system. The underlying assumption of this procedure developed by Pavlovsky in 1935 (Pavlovsky 1956 and Harr 1962) is that equipotential lines at various critical locations in the flow region can be approximated by straight vertical lines. These equipotential lines divide the flow region into parts or fragments. Other assumptions inherent in the method of fragments procedure are (a) Darcy's law is valid, (b) steady-state flow exists, and (c) the soil medium is approximated as a single homogeneous and isotropic layer or at series of such layers. The transformation of anisotropic soil to an equivalent isotropic soil is described in Section 4.7 of this manual.

b. Basic Concepts. The quantity of flow through a single fragment is computed as:

$$q = \frac{kh_i}{\phi_i} \quad (B-1)$$

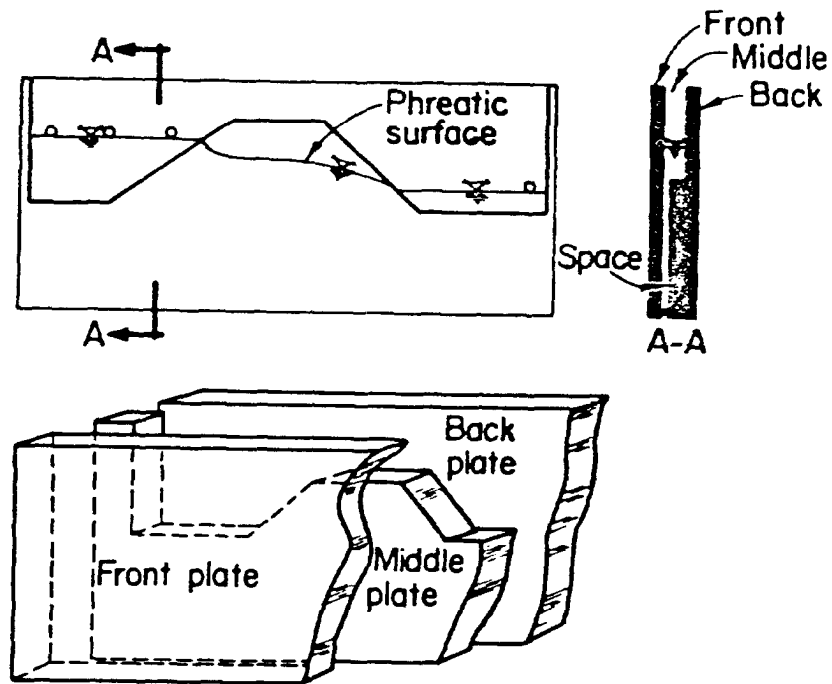
where

k - coefficient of permeability

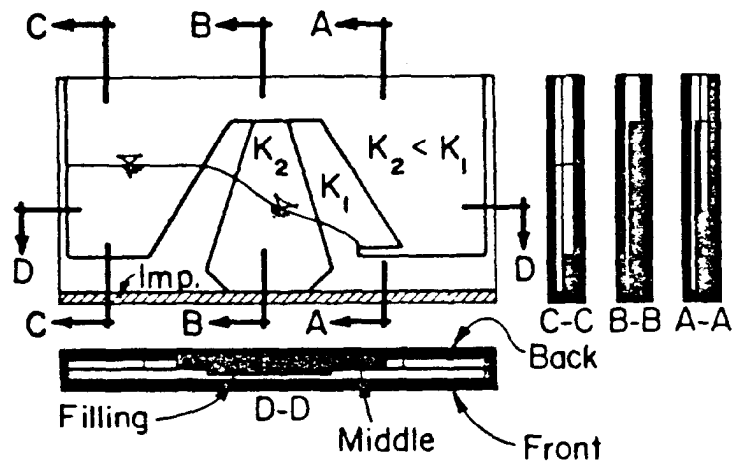
h_i = head loss through the fragment

ϕ_i = dimensionless form factor, = N_e/N_f

30 Sep 86



a. Homogeneous earth dam



b. Zoned earth dam

Figure B-3. Viscous flow model (courtesy of Bear¹⁴⁰)

30 Sep 86

Because the fragment boundaries consist of equipotential lines, the flow through each fragment must be equal to the total flow through the system. Thus

$$Q = \frac{kh_1}{\phi_1} = \frac{kh_2}{\phi_2} = \dots = \frac{kh_n}{\phi_n} \quad (B-2)$$

Since summation of the head loss in each fragment is equal to the total head loss, the total quantity of flow can be expressed as

$$Q = \frac{kh}{\sum_{i=1}^n \phi_i} \quad (B-3)$$

where h is the total head loss through the section. Along the same line, the head loss in each fragment can be calculated from

$$h_i = \frac{h\phi_i}{\sum_{i=1}^n \phi_i} \quad (B-4)$$

The head loss along any impermeable boundary of a fragment is assumed to change linearly. Thus the head loss within fragment i up to point A is equal to the head loss in the fragment times the ratio of the length of the boundary to point A to the total length of boundary. The basic concept of the method of fragment procedure is to break the flow region into parts for which the form factor is shown in figure B-4 (Harr 1977). This manual will describe how to calculate the factors for each type of fragment (Harr 1962 and Harr 1977).

c. Fragment Types. There are currently nine different fragment types. Of these, the first six are for confined flow while the last three are for unconfined flow.

(1) Type I. This fragment type represents a region of parallel horizontal flow between impervious boundaries. For this internal type fragment, shown in figure B-5a, the flow per unit width is equal to

$$Q = \frac{kh_i a}{L} \quad (B-5)$$

30 Sep 86

Thus from Equation B-1, the form factor is

$$\phi = \frac{L}{a} \quad (\text{B-6})$$

An elemental Type I section shown in figure B-5b illustrates that

$$d\phi = \frac{dx}{y} \quad (\text{B-7})$$

This elemental section will be used to derive the form factors for fragment types IV, V, and VI.

(2) Type II. This fragment type represents a vertical impervious boundary embedded a length S into a pervious layer of thickness T . This fragment can represent either an entrance condition (figure B-6a) or an exit condition (figure B-6b). The form factor is obtained from the plot in figure B-4 where the scale of ϕ is given as one-half the reciprocal of

Q/kh or

$$\phi = \frac{1}{2} \left(\frac{kh}{Q} \right) \quad (\text{B-8})$$

The form factor could also be expressed as the ratio of the elliptic integral of the first kind with modulus m over the elliptic integral of the complementary modulus, m' . For this fragment type, the modulus value is a function of the ratio S/T . The graph in figure B-7 was obtained by solving the elliptic integrals for various combinations of S/T . For the type II fragments, the ratio of b/T equals 0.

(3) Type III. This type of fragment represents an impervious layer of length b , a vertical boundary of depth S , in a pervious layer of thickness T . Either of the sections shown in figure B-8 can represent this fragment type. The form factor is obtained directly from figure B-7 with b/T other than zero. For this case, the elliptic integral modulus is a function of both b/T and S/T .

(4) Type IV. This type is an internal fragment with boundary length b , embedment length S , in a pervious layer of thickness T . Figure B-9a illustrates the two possible configurations. Pavlovsky divided the flow region into active and passive parts based on the results of electrical analogue tests as shown in figure B-9b by line AB. An angle of 45 deg was assumed for the line dividing the two parts of the fragment. This resulted in two cases, depending on the relation between b and S . For the case where $b \leq S$, the

Fragment type	I	Form factor, Φ (h is head loss through fragment)	Fragment type	V	Form factor, Φ (h is head loss through fragment)
Illustration		$\Phi = \frac{L}{a}$	V		$L \leq 2s:$ $\Phi = 2 \ln \left(1 + \frac{L}{2a} \right)$ $L \geq 2s:$ $\Phi = 2 \ln \left(1 + \frac{s}{a} \right) + \frac{L-2s}{L}$
II		$\Phi = \frac{1}{2} \left(\frac{Ah}{Q} \right)$, Fig. 5-13	VI		$L \geq s' + s'':$ $\Phi = \ln \left[\left(1 + \frac{s'}{a'} \right) \left(1 + \frac{s''}{a''} \right) \right] + \frac{L - (s' + s'')}{L}$ $L \leq s' + s'':$ $\Phi = \ln \left[\left(1 + \frac{b'}{a'} \right) \left(1 + \frac{b''}{a''} \right) \right]$ where $b' = \frac{L + (s' - s'')}{2}$ $b'' = \frac{L - (s' - s'')}{2}$
III		$\Phi = \frac{1}{2} \left(\frac{Ah}{Q} \right)$, Fig. 5-13	VII		$\Phi = \frac{2L}{h_1 + h_2}$ $Q = k \frac{h_1^2 - h_2^2}{2L}$
IV		$b \leq s:$ $\Phi = \ln \left(1 + \frac{b}{a} \right)$ $b \geq s:$ $\Phi = \ln \left(1 + \frac{s}{a} \right) + \frac{b-s}{L}$	VIII		$Q = k \frac{h_1 - h_2}{\cot \alpha} \ln \frac{h_d}{h_d - h}$
IX		$Q = k \frac{a_2}{\cot \beta} \left(1 + \ln \frac{a_2 + h_2}{a_2} \right)$	IX		$Q = k \frac{a_2}{\cot \beta} \left(1 + \ln \frac{a_2 + h_2}{a_2} \right)$

Figure B-4. Summary of fragment types and form factors (courtesy of McGraw-Hill Book Company 181)

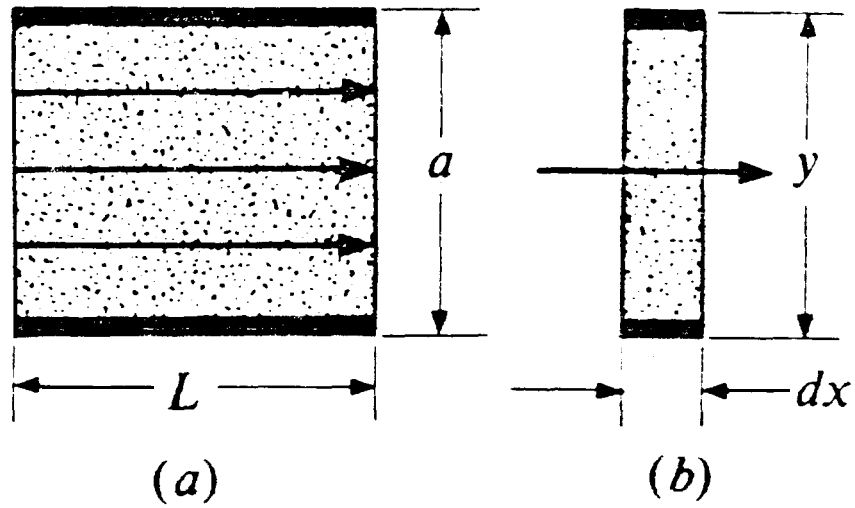


Figure B-5. Type I fragment (courtesy of McGraw-Hill Book Company¹⁸¹)

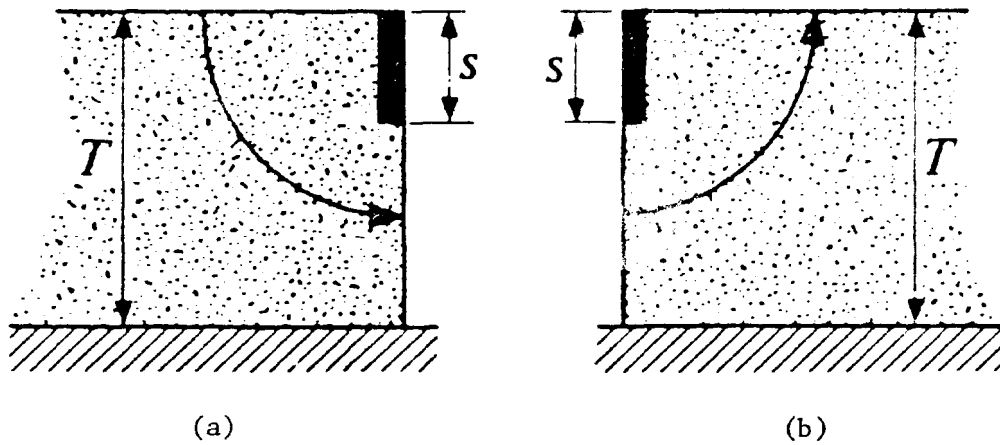
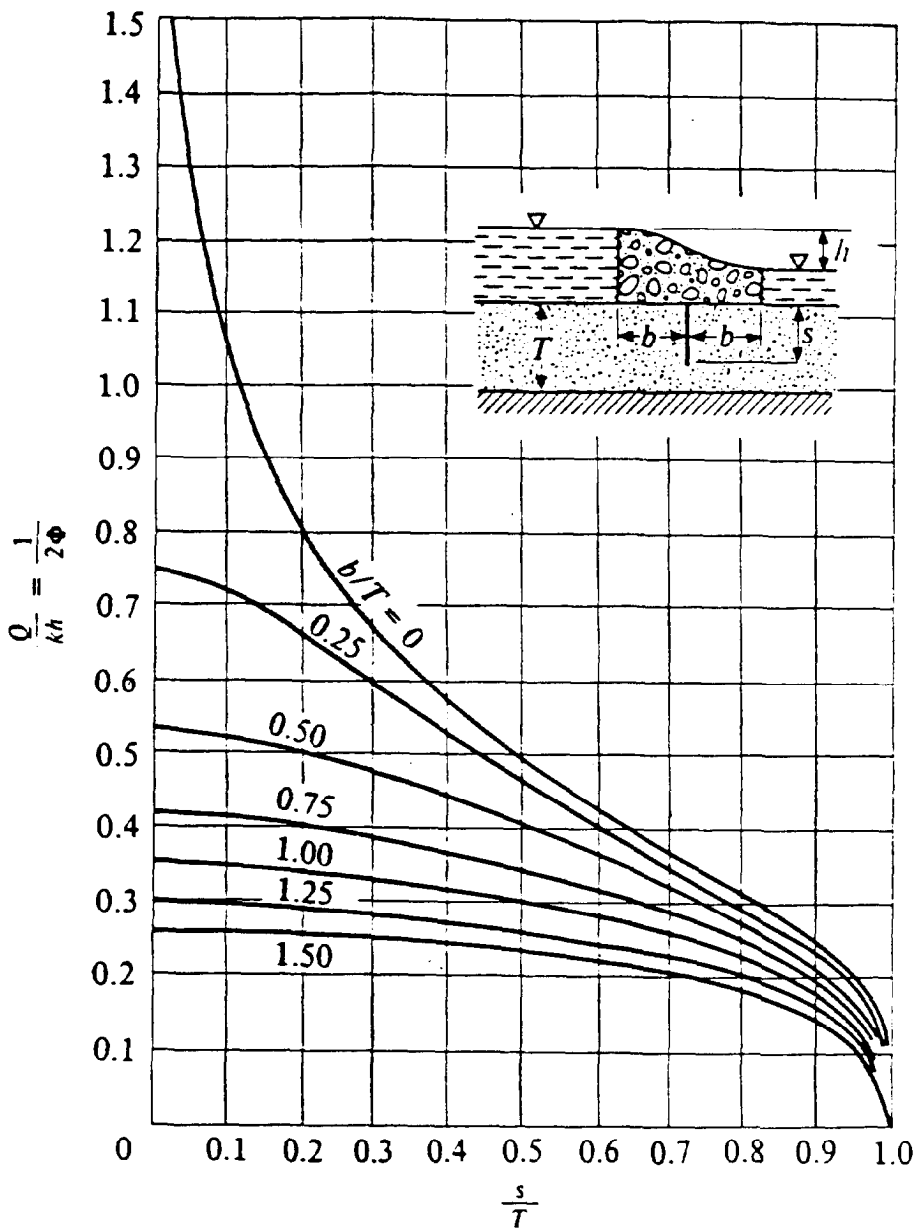


Figure B-6. Type II fragment (courtesy of McGraw-Hill Book Company¹⁸¹)

30 Sep 86



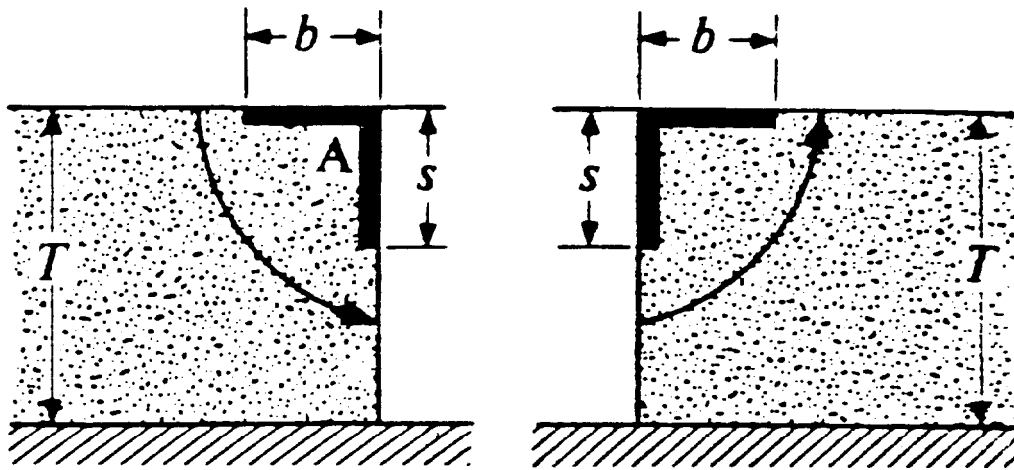
$$\text{If } m = \cos \frac{\pi s}{2T} \sqrt{\tanh^2 \frac{\pi b}{2T} + \tan^2 \frac{\pi s}{2T}}$$

$$\text{for } m \leq 0.3, \frac{Q}{kh} = \frac{1}{\pi} \ln \frac{4}{m}$$

$$\text{for } m^2 \geq 0.9, \frac{Q}{kh} = \frac{-\pi}{2 \ln \left(\frac{1-m^2}{16} \right)}$$

Figure B-7. Quantity of discharge for symmetrically placed pilings (courtesy of McGraw-Hill Book Company¹⁸¹)

30 Sep 86



(a)

(b)

Figure B-8. Type III fragment (courtesy of McGraw-Hill Book Company 181)

active zone is composed of elements of type I fragments of width dx illustrated in figure B-9c. The form factor is the integral of dx over y from 0 to b which results in a form factor of

$$\phi = \ln \left(1 + \frac{b}{a} \right) \quad (\text{B-9})$$

If $b \geq S$, then the fragment can be divided into two fragments as shown in figure B-9e. The first is a type IV with $b \geq S$ and the second is a type I fragment with L equal to $b - S$. Thus the form factor is the sum of the form factors which would be

$$\phi = \ln \left(1 + \frac{S}{a} \right) + \frac{b - S}{T} \quad (\text{B-10})$$

(5) Type V. This fragment type has two vertical boundaries of equal embedment S in a pervious layer of thickness T . As shown in figure B-10, the form factor for this fragment is twice that for the type IV fragment.

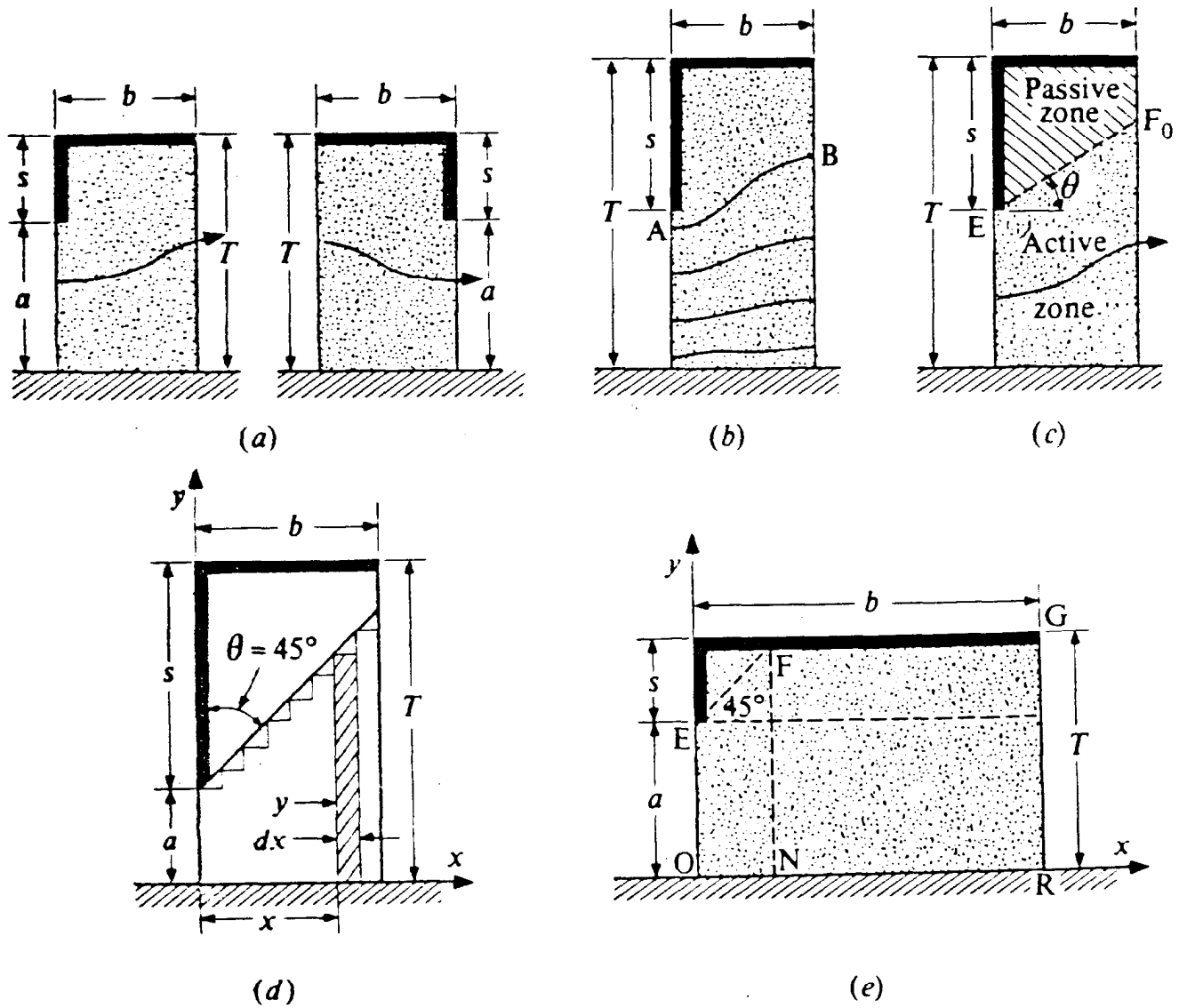


Figure B-9. Type IV fragment (courtesy of McGraw-Hill Book Company¹⁸¹)

30 Sep 86

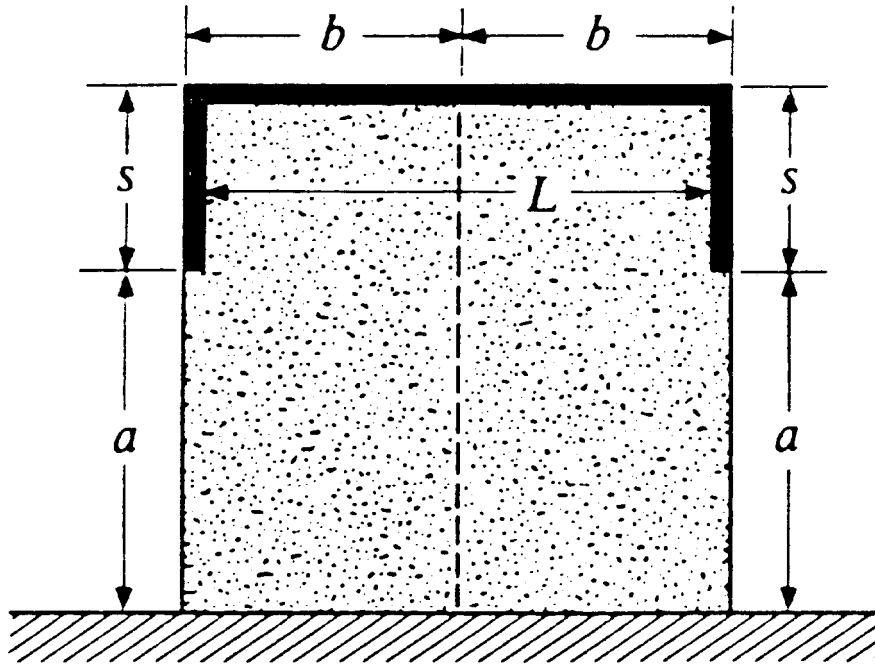


Figure B-10. Type V fragment (courtesy of McGraw-Hill Book Company¹⁸¹)

Since there were two cases of type IV fragment, there are two cases for the type V fragment. The two cases are for $L \leq 2s$ and $L \geq 2S$. For the first case, the form factor is

$$\phi = 2\ell n\left(1 + \frac{L}{2a}\right) \tag{B-11}$$

For the second case which consists of a type I fragment within two type IV fragments, the form factor is

$$\phi = 2\ell n\left(1 + \frac{S}{a}\right) + \frac{L - 2S}{T} \tag{B-12}$$

(6) Type VI. This fragment type, illustrated in figure B-11, is the same as the type V fragment except that the embedment lengths are different. Using the same approximations as in fragment type IV, there are two cases for the form factor. For the first case where $L > (S' + S'')$, the form factor is

$$\left[\left(1 + \frac{S'}{a'}\right)\left(1 + \frac{S''}{a''}\right)\right] + \frac{L - (S' + S'')}{T} \tag{B-13}$$

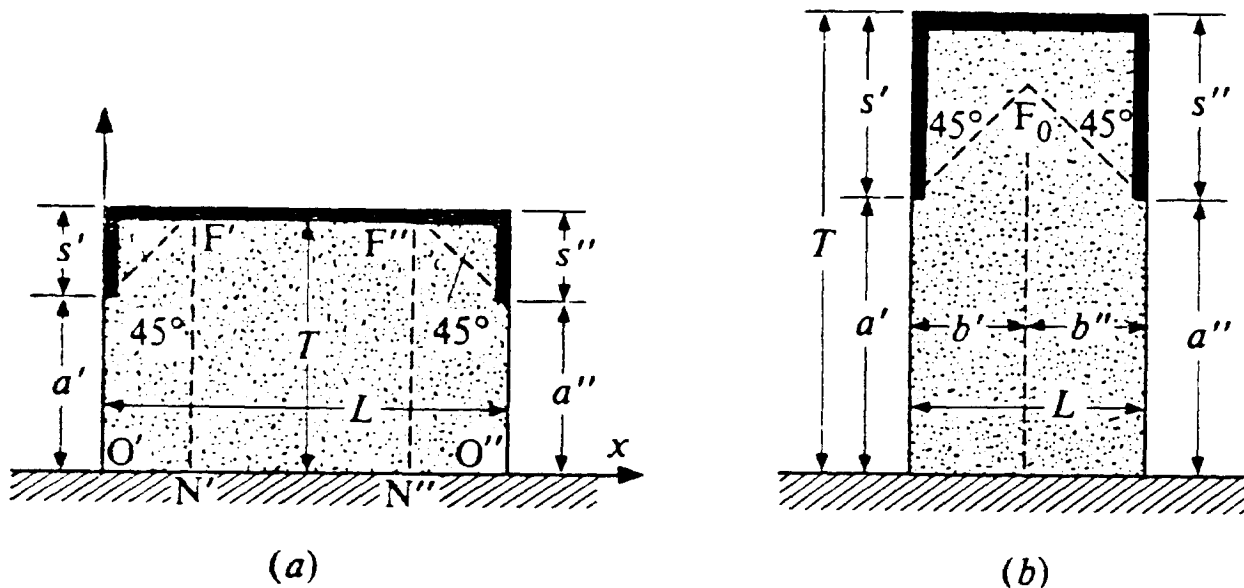


Figure B-11. Type VI fragment (courtesy of McGraw-Hill Book Company¹⁸¹)

For the second case where $L \leq (S' + S'')$, the form factor is

$$\phi = \ln \left[\left(1 + \frac{b'}{a'} \right) \left(1 + \frac{b''}{a''} \right) \right] \quad (\text{B-14})$$

where

$$b' = \frac{L + (S' - S'')}{2}$$

$$b'' = \frac{L - (S' - S'')}{2}$$

(7) Type VII. This fragment represents the condition of unconfined flow. This flow is characterized by having one boundary of the flow domain as a free surface (line AB in figure B-12). This free surface separates the saturated region from that region where no flow occurs. From Darcy's law and Dupuit's assumptions, the hydraulic gradient is $(h_1 - h_2)/L$ and the cross-sectional area is $(h_1 + h_2)/2$, thus the flow is

$$Q = k \frac{h_1^2 - h_2^2}{2L} \quad (\text{B-15})$$

30 Sep 86

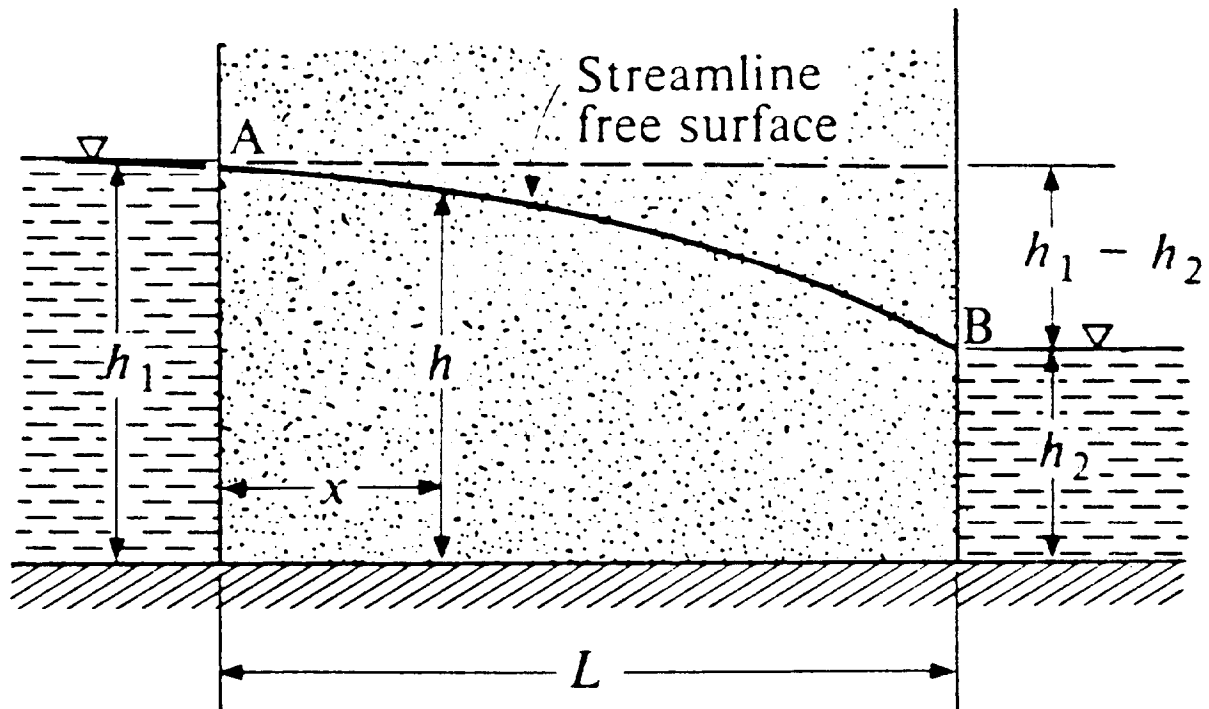


Figure B-12. Type VII fragment (courtesy of McGraw-Hill Book Company¹⁸¹)

From this, the form factor is

$$\phi = \frac{2L}{h_1 + h_2} \quad (\text{B-16})$$

(8) Type VIII. This fragment type represents an upstream slope entrance condition on an earth dam of height h_d and is illustrated in figure B-13. It was assumed that the curve streamlines (cd) could be approximated by horizontal flow channels of length ed (Pavlovsky 1956 and Harr 1977). With this assumption, the hydraulic gradient in each channel is

$$i = \frac{d(h_1 - h)}{dy} = \frac{a_1}{\cot \alpha (h_d - y)} \quad (\text{B-17})$$

30 Sep 86

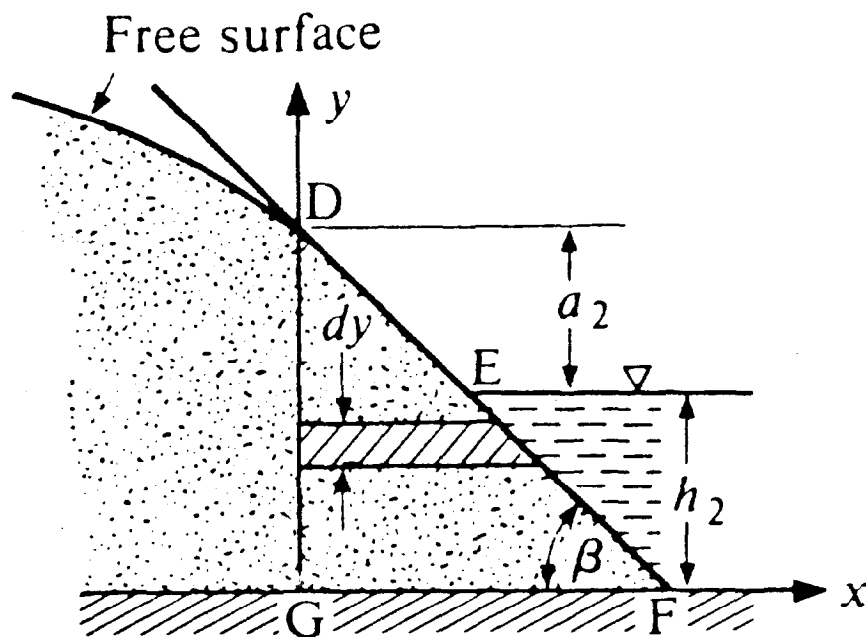


Figure B-14. Type IX fragment (courtesy of McGraw-Hill Book Company¹⁸¹)

d. Exit Gradient. The method of fragments procedure can be used to determine the exit gradient discussed in paragraph 4.9 of this manual. For this procedure, the last fragment (downstream) needs to be either a type II or a type III fragment. The exit gradient is defined as (Harr 1962)

$$I_E = \frac{h_m \pi}{2KT_m} \quad (\text{B-20})$$

where

h_m = head loss in the last fragment

K = complete elliptic integral of the first kind with modulus m

T = depth of flow region

As defined before, the modulus m is a function of both b/T and S/T and is defined as

$$m = \cos \frac{\pi S}{2T} \sqrt{\tanh^2 \frac{\pi b}{2T} + \tan^2 \frac{\pi S}{2T}} \quad (\text{B-21})$$

30 Sep 86

Instead of calculating the various values, for type II fragments figure B-15 can be used with S/T to obtain the fraction for $I_E S/h_m$. By substituting the appropriate values, the exit gradient is calculated.

e. Example 1. The method of fragment procedure for confined flow will be illustrated in the following example obtained for John H. Overton Lock and Dam (U. S. Army Engineer District, St. Louis 1978). This problem will analyze the steady state flow conditions for a two-dimensional idealization of the lock structure. The quantity of flow and head along the bottom of the lock will be determined. For illustrative purposes, the exit gradient procedure will be included. The dimensions of the structure, shown in figure B-16, are those used in the analysis after the cross section has been transformed to account for soil anisotropy. The original analysis contained two soil layers, but for illustrative purposes the soil will be modeled as one layer. The first step is to determine the form factors for each region. The first region is a type II fragment with $S = 19$ ft and $T = 89$ ft. Using figure B-7 with $S/T = 0.21$, the fraction for $Q/kh = 0.78$, thus $\Phi_1 = 0.641$. Region 2 is a type I fragment with $L = 456$ ft and $a = 70$ ft. From figure B-4, the form factor for the type I fragment is equal to L/a , thus $\Phi_2 = 6.514$. The third region is a type II fragment with $S = 9$ ft and $T = 79$ ft. Using figure B-7 with $S/T = 0.114$, the fraction for $Q/kh = 1.01$, thus $\Phi_3 = 0.495$. The summation of the form factors is 7.650. The quantity of flow is calculated from equation B-3. Using transformed permeability of 400×10^{-4} cm/sec and a total head of 18 ft, the quantity of flow is calculated to be 266.8 ft³/day/foot of lock width. The head loss in each fragment is calculated from equation B-4. The following table lists the head loss for each fragment in this problem:

<u>Region</u>	<u>Φ</u>	<u>h_i</u>
1	0.641	1.51
2	6.514	15.33
3	<u>0.495</u>	<u>1.16</u>
	$\Sigma = 7.650$	$\Sigma = 18.00$

The head along the bottom decreases from 16.49 ft at the upstream end to 1.16 at the downstream end. Using the assumption of a linear distribution of the head loss within a fragment, the head at any point along the bottom of the lock could be calculated as

$$\text{head at pt a} = 16.49 \text{ ft} - \left(\frac{\text{distance to pt A for upstream of lock}}{\text{total length of lock}} \right) 15.33 \text{ ft} \quad (\text{B-22})$$

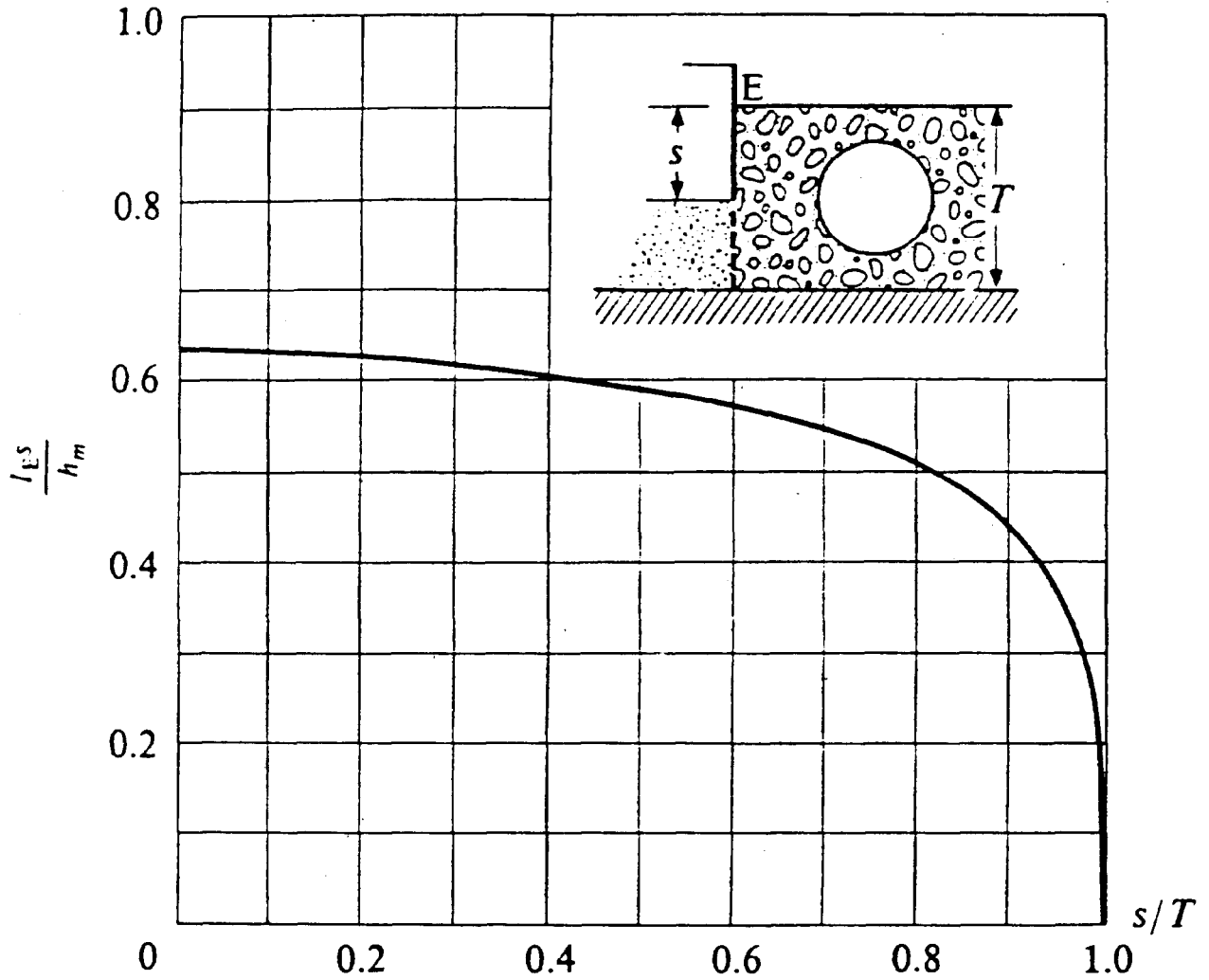


Figure B-15. Relationship for determining the exit gradient as a function of the head loss in the fragment and geometry for a Type II fragment (courtesy of McGraw-Hill Book Company¹⁸¹)

30 Sep 86

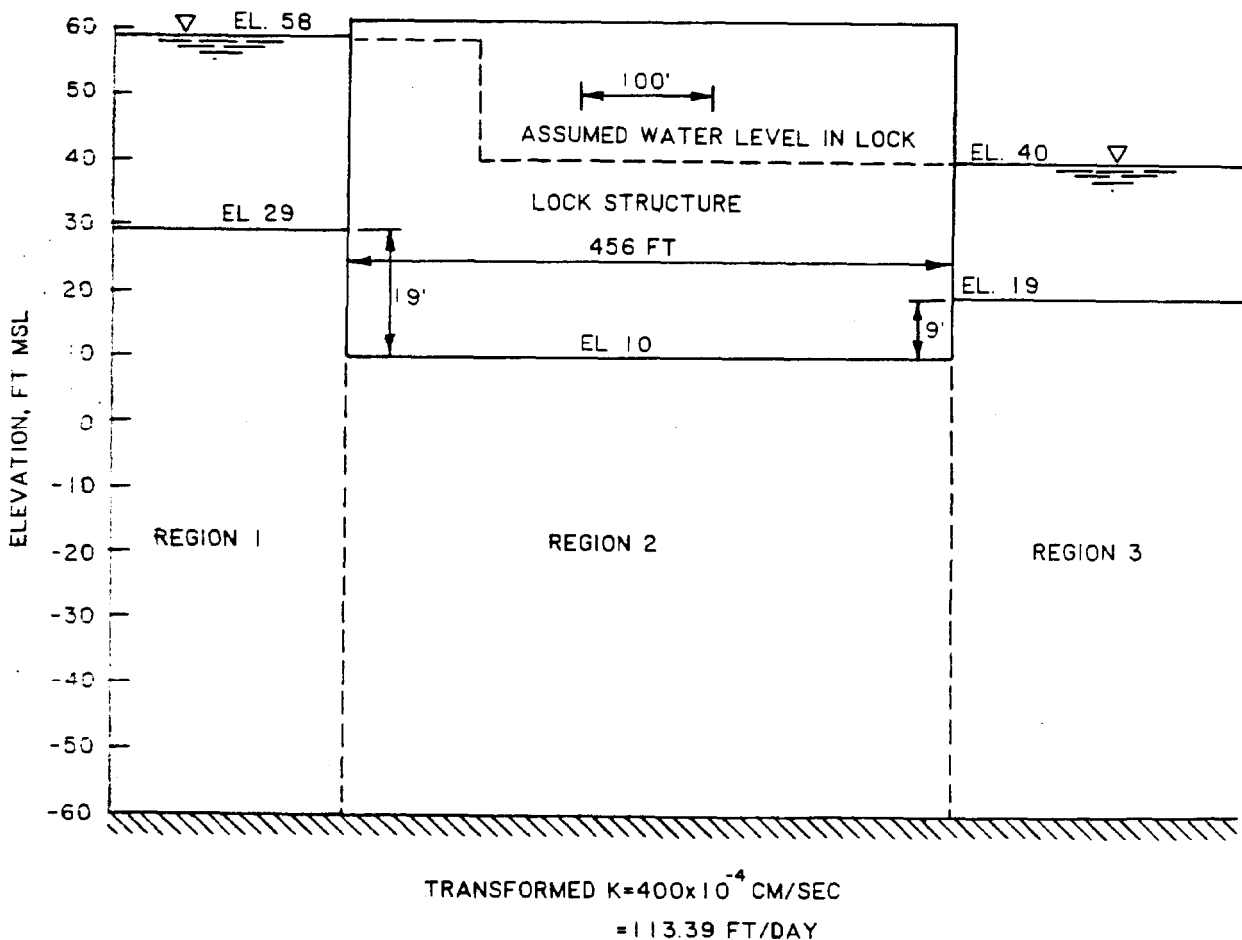


Figure B-16. Transformed section of John H. Overton Lock simplified to one soil layer (from U. S. Army Engineer District, St. Louis¹¹²)

The exit gradient is calculated for region 3 which is a type II fragment. Using $S/T = 0.114$ with figure B-15, the fraction for $I_E S/h_m$ is found to be 0.63. With a head loss of 1.16 ft in this fragment, the exit gradient is calculated to be 0.082.

f. Example 2. This example will illustrate the method of fragment procedure for unconfined flow problems. The example is obtained from John H. Overton Lock and Dam (U. S. Army Engineer District, St. Louis 1978). The problem is to locate the free surface in the closure dam and to determine the quantity of flow through the dam under steady state conditions. The dimensions of the structure shown in figure B-17 are after the material has been transformed to account for soil anisotropy. This sample problem assumes an impervious boundary at the base of the dam. To account for some flow under the dam, the impervious boundary could be lowered. By lowering the boundary to the lowest possible point, bounds for the problem would be established. There are three fragment types in this earthen embankment. Region 1 is a

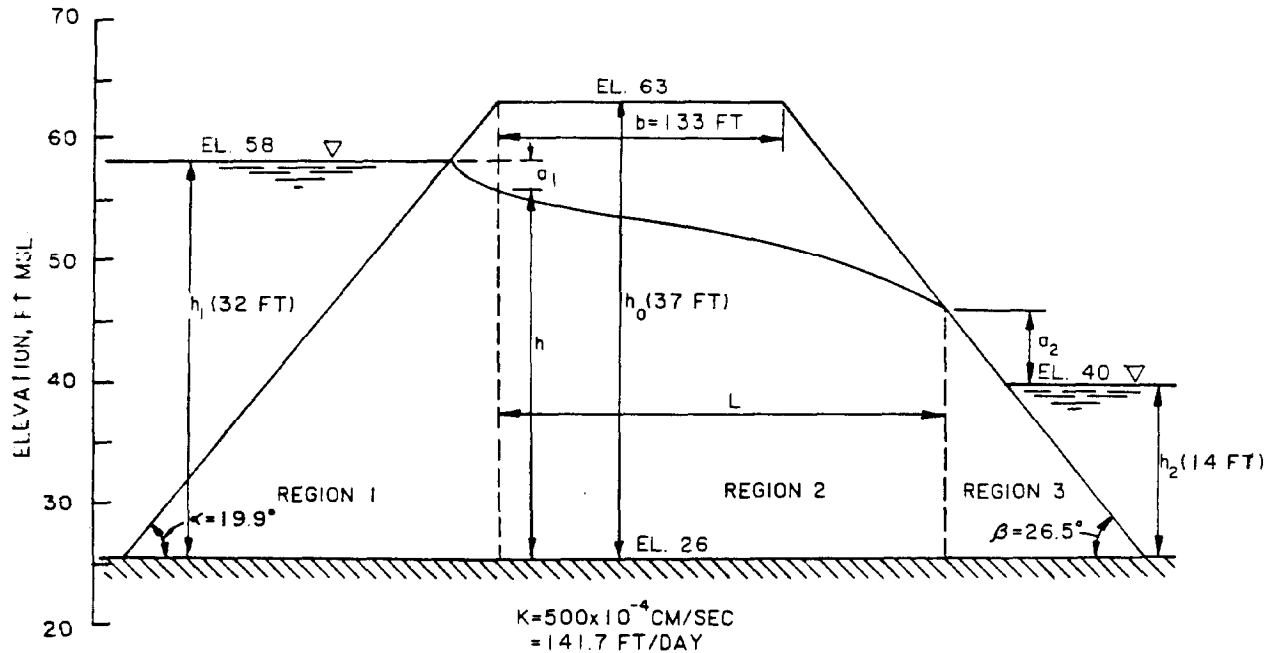


Figure B-17. Transformed section of John H. Overton closure dam (from U. S. Army Engineer District, St. Louis¹¹²)

type VIII fragment while region 2 is a type VII fragment and region 3 is a type IX fragment. To calculate the flow through region 1, equation B-18 is used with $h_i = 32$ ft; $h_d = 37$ ft, and $\alpha = 19.9$ deg ($\cot \alpha = 2.76$).

Substituting into the equation produces

$$\frac{Q}{k} = \frac{32 - h}{2.76} \ln \frac{37}{37 - h} \quad (B-23)$$

For region 2, the quantity of flow is calculated from equation B-15. Substituting into this equation produces

$$\frac{Q}{k} = \frac{h^2 - (a_2 + 14 \text{ ft})^2}{2L} \quad (B-24)$$

For region 3, equation B-19 defines the quantity of flow. By substituting $\cot \beta = 2$ and $H_2 = 14$ ft produces

$$\frac{Q}{k} = \frac{a_2}{2} \left(1 + \ln \frac{a_2 + 14}{a_2} \right) \quad (B-25)$$

30 Sep 86

From the embankment geometry, L can be defined as

$$L = b + \cot \beta [h_d - (a_2 + h_2)] \quad (B-26)$$

By substituting into equation B-26, there are four equations with four unknowns, h , a_2 , Q/k , and L . There are several methods to solve these four equations (Harr 1977). For the case where $h_2 = 0$, a reduction of two equations and two unknowns occurs. For this example, equation B-23 will be combined with equation B-24 and equation B-26 will be substituted for L . This produces

$$\frac{32 - h}{2.76} \ln \left(\frac{37}{37 - h} \right) = \frac{h^2 - (a_2 + 14)^2}{2[133 + 2[37 - (a_2 + 14)]]} \quad (B-27)$$

Also equation B-23 can be combined with equation B-25, producing

$$\frac{32 - h}{2.76} \ln \left(\frac{37}{37 - h} \right) = \frac{a_2}{2} \left(1 + \ln \frac{a_2 + 14}{a_2} \right) \quad (B-28)$$

Equations B-27 and B-28 have reduced the equations and unknowns by two. Thus with two equations and two unknowns, a trial and error graphical process can be used. The results of this process are shown in figure B-18 and indicate that $h = 28.9$ ft and $a_2 = 0.9$ ft., Substituting into equations B-23 and B-25 generates a Q/k value of 1.71 which results in an estimated flow of 242.4 ft³/day/ft of dam. Knowing h and a_2 , the location of the phreatic surface can be estimated.

9. Flow in Layered Systems. One of the limitations of the method of fragments is that the flow layer is assumed to be homogeneous and isotropic. An approximate procedure to determine flow characteristics of a layered system was proposed by Polubarinova-Kochina (1941). Harr (1977) extended this method as follows. The coefficients of permeability for the two layers are related by a dimensionless parameter ϵ by the expression

$$\tan \pi \epsilon = \sqrt{\frac{k_2}{k_1}} \quad (B-29)$$

where

k_1 = coefficient of permeability of the upper layer

k_2 = coefficient of permeability of the lower layer

30 Sep 86

$$\frac{32 - h}{2.76} \ln \left(\frac{37}{37 - h} \right) = \frac{h^2 - (a_2 + 14)^2}{2(133 + 2[37 - (a_2 + 14)])}$$

Equation B-27

<u>h</u>	<u>a₂</u>
28.8	-0.4
29.0	2.1
30.0	8.6
31.0	13.6

$$\frac{32 - h}{2.76} \ln \left(\frac{37}{37 - h} \right) = \frac{a_2}{2} \left(1 + \ln \frac{a_2 + 14}{a_2} \right)$$

Equation B-28

<u>h</u>	<u>a₂</u>
29.9	0.6
27.8	1.2
25.6	1.7

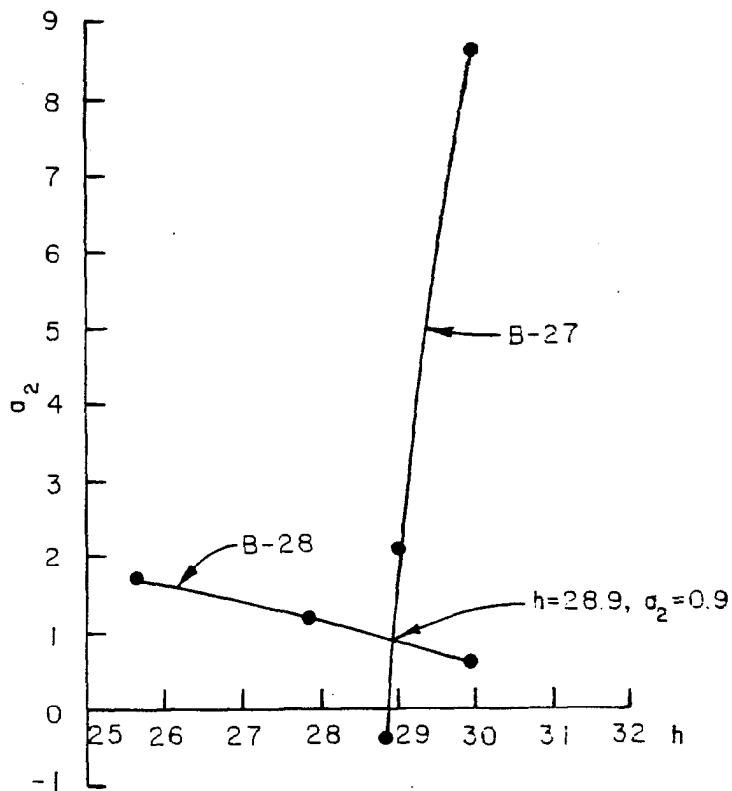


Figure B-18. Graphical solution-of equations B-27 and B-28
(from U. S. Army Engineer District, St. Louis¹¹²)

30 Sep 86

The ratio of permeabilities can vary from 0 to infinity. Over this range, ϵ ranges from 0 to 1/2. The basis of this method is to determine the flow and head losses for three certain special cases of ϵ and then interpolate between these values. The three special cases are as follows:

(1) $\epsilon = 0$. For ϵ to be equal to 0, k_2 must equal 0. Therefore the problem is reduced to a one-layer problem with a flow region thickness equal to the upper layer.

(2) $\epsilon = 1/4$. For ϵ to be equal to 1/4, k_2 must equal k_1 . Therefore, the problem is reduced to a one-layer problem with a flow region the thickness of the upper and lower layers.

(3) $\epsilon = 1/2$. For ϵ to be equal to 1/2, k_2 must be infinite. This case represents the infinite flow where there is no resistance to flow in the lower layer. Since $Q/k_2h = \infty$ the inverse of this ratio is equal to zero.

This procedure can be expanded to a three-layer system by the use of two ϵ values. The first value would be for the top two layers, while the second would be for the bottom two layers.

h. Example 3. This example will illustrate the method of fragment procedure for confined flow in a two-layer system. The example is obtained from John H. Overton Lock and Dam (U. S. Army Engineer District, St. Louis 1978). This problem will analyze the steady-state flow conditions for the dam and stilling basin. The quantity of flow and head along the bottom of the structure will be determined. For illustrative purposes, the exit gradient procedure will be included. The effect of various parameters like the length of sheetpile cutoff can be studied using this procedure. The dimensions of the structure, shown in figure B-19, are those used in the analysis after the cross section has been transformed to account for soil anisotropy. There are three fragments for this problem and three ϵ cases to be evaluated. For the first case, $\epsilon = 0$, all the flow is assumed to occur in the clay layer. Region 1 is a type II fragment with $S = 25$ ft and $T = 35$ ft. Using figure B-7 with $S/T = 0.71$, the fraction for $Q/kh = 0.36$, thus $\phi_1 = 1.38$. The second region is a type V fragment with $S = 13$ ft, $T = 23$ ft, and $L = 73.5$ ft. Since $L > 25$, equation B-13 is used to calculate the form factor. For the above values, the form factor is 3.73. Region 3 is a type II fragment where $S = 24$ ft and $T = 34$ ft. The form factor, using figure B-7, is calculated to be 1.36. Using equation B-1, the ratio Q/k_1 is 2.78 and k_1/Q is 0.36 .

For the second case, $\epsilon = 1/4$, the flow is assumed to be equal in both layers. The form factors are recalculated using the same fragment types. The value of Q/k_1 is 6.50 which results in a k_1/Q value of 0.15. For the last case, $\epsilon = 1/2$, all flow is assumed to be in the lower sand layer. Only vertical flow occurs in the top or clay layer. For this case, Q/k_1 is infinite which results in a k_1/Q of 0 . A plot of k_1/Q versus ϵ is shown in figure B-20a. For this problem k_2 is 200 times k_1 , therefore ϵ equals 0.48.

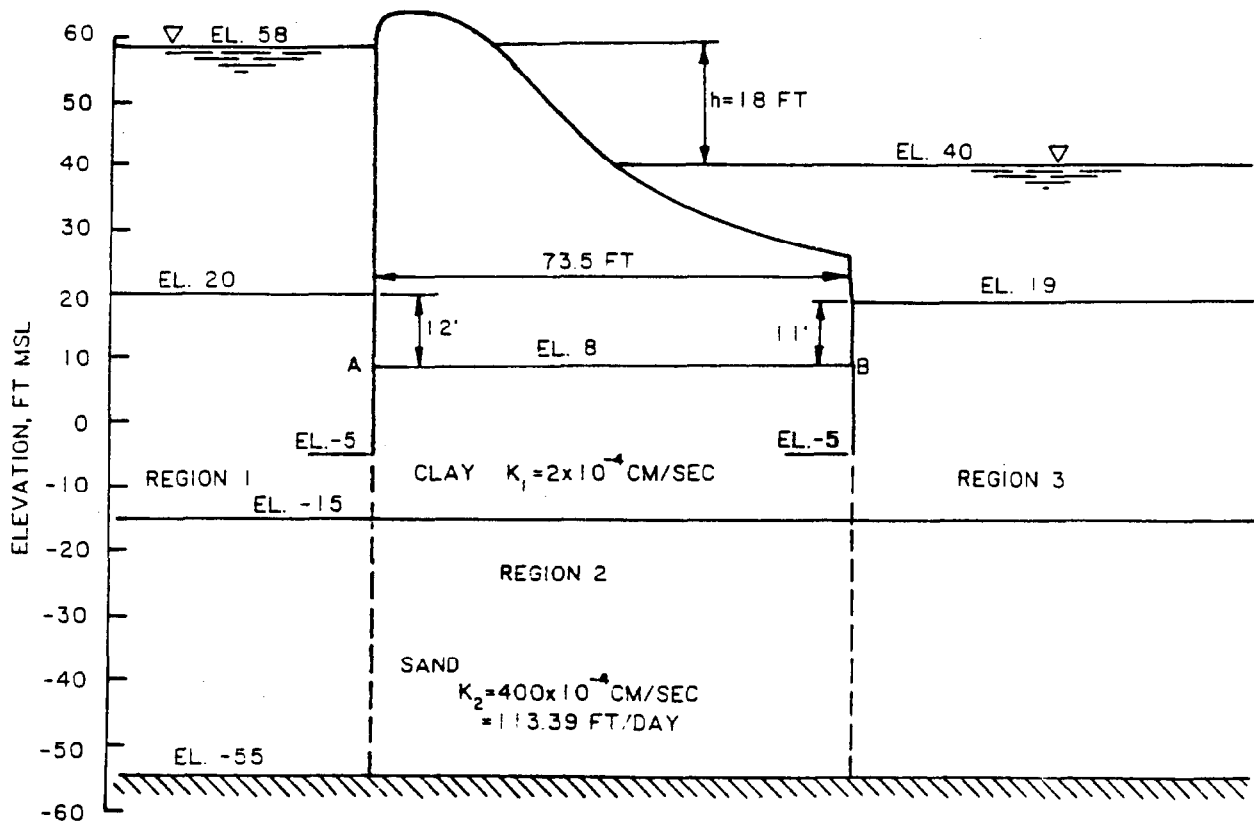


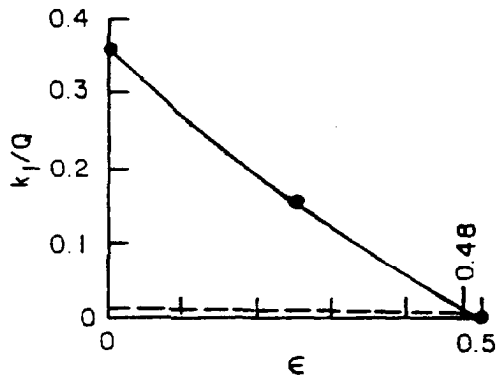
Figure B-19. Transformed section of John B. Overton Dam and stilling basin for one case of sheet pile lengths (from U. S. Army Engineer District, St. Louis¹¹²)

By interpolation for $\epsilon = 0.48$, k_1/Q equals 0.01 which results in a flow Q of $56.7 \text{ ft}^3/\text{day}/\text{ft}$ of dam. To determine the head along the bottom of the structure, the head at points A and B in figure B-19 must be determined. Using the procedure described in example 1, equation B-22, the following head loss and total head values are calculated.

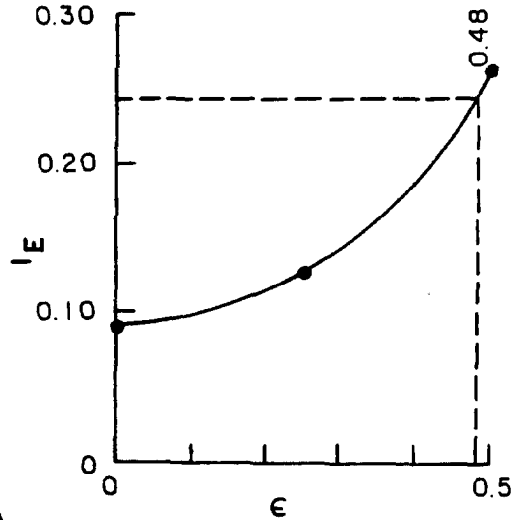
ϵ	Point A		Point B	
	Head Loss ft	Total Head ft	Head Loss ft	Total Head ft
0	5.2	52.8	12.8	45.2
1/4	6.2	51.9	12.0	46.0

For the case where $\epsilon = 1/2$, the head anywhere along the bottom of the structure is equal to half the total head loss, or for this case 9 ft. Thus the total head on points A and B is equal to 49 ft. Figure B-20b is the plot of the total head versus ϵ and shows, for an ϵ of 0.48, the total head at point A is 49.4 ft while the total head at point B is 48.5 ft. The exit gradient for each ϵ case is calculated by the procedure described in example 1. For the case of $\epsilon = 0$, the fraction $I_E S/h_m$ is 0.55 which with $S = 24 \text{ ft}$

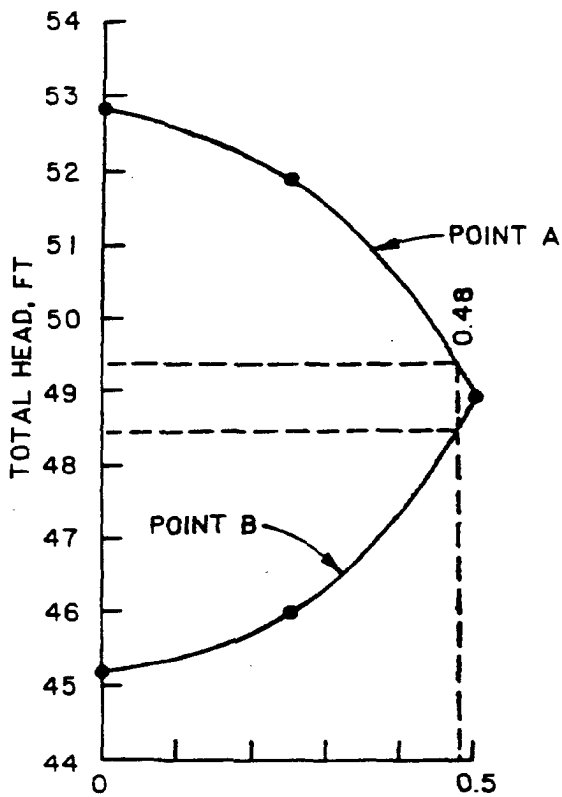
30 Sep 86



(A)



(C)



(B)

Figure B-20. ϵ value plots for John H. Overton Dam and stilling basin (from U. S. Army Engineer District, St. Louis¹¹²)

30 Sep 86

and $h_m = 3.8$ ft produces $I_E = 0.087$. For the $\epsilon = 1/4$ case, the fraction $I_E S/h_m$ is 0.615 which with $S = 24$ ft and $h_m = 5.0$ ft produces $I_E = 0.128$. For the case where $\epsilon = 1/2$, the head loss is the total head and the distance is the thickness of the top layer. Using the equation

$$I_E = \frac{h_m}{2d_1} \quad (B-30)$$

the exit gradient is 0.265. The exit gradient versus ϵ plot is shown in figure B-20c. For an ϵ value of 0.48, the exit gradient is 0.245.

i. Uses and Limitations. The method of fragment procedure should be used as a design tool where various factors are changed to evaluate their effect or as an analytical tool when quick approximate results are needed. When numerous factors are varied, the construction of flow nets becomes very tedious and time consuming. The method of fragment procedure will generate reasonable results for problems where the assumptions are not greatly violated. There are several points the user needs to be aware of when using this procedure. The flow region must be generalized so that it consists of horizontal and vertical boundaries. The procedure models the actual flow paths within the flow region, thus if there is any doubt as to the direction, a rough flow net should be drawn. This becomes important when a small portion of a structure is modeled with several fragments because the flow could be modeled in unnatural paths. The accuracy of the results is dependent upon how well the fragment boundary actually represents vertical equipotential lines. The greater the deviation, the greater the degree of error. However, for many practical problems reasonable results are generated. Comparison of the method of fragment results with finite element solutions for a one-layer system showed that the quantity of flow values for the fragment procedure are within 8 percent of the finite element results, while the uplift values are within 38 percent of the finite element results. The Computer-Aided Structural Engineering (CASE) project has developed a computer program for the method of fragments procedure with a user manual describing the program (Pace et al. 1984).

B-6. Finite Difference Method.

a. Method of Solution. As previously mentioned in Chapter 4, the finite difference method solves the Laplace equations by approximating them with a set of linear algebraic expressions. The approximation is mathematical rather than physical. The early methods of solving finite difference expressions for Laplace's equation were based upon hand calculations by the relaxation method⁽¹⁾. However, more recently a wide range of finite difference solutions suited to the digital computer have been developed. A description of

(1) For example, see Appendix A of EM 1110-2-2501.

30 Sep 86

available methods used to solve finite difference problems including example applications, case studies, and computer program listings is available (Rushton and Redshaw 1979).

b. Advantages. Use of iterative techniques such as successive over-relaxation which converge to the correct solution allows solution of unconfined and transient flow problems. For simple problems, the finite difference method is usually more economical than the finite element method (Rushton and Redshaw 1979).

c. Disadvantages. The finite difference method is not suited to complex geometry, including sloping layers and pockets of materials of varying permeability. Irregular grids are difficult to input. Therefore, zones where seepage gradients or velocities are high cannot be accurately modeled (Rushton and Redshaw 1979).

d. Applications. The finite difference method was used at WES to simulate seepage conditions in streambanks induced by sudden drawdown of the river level. As mentioned previously, this study included a viscous flow model, field observations, and application of the finite element and finite difference methods. The results of the study indicated that the finite difference method provided satisfactory and economical solutions for transient unconfined fluid flow in porous, anisotropic, and nonhomogeneous media (Desai 1970 and Desai 1973). The finite difference method was used to predict the location of the phreatic surface within a zoned embankment with arbitrary fluctuations of the reservoir (Dvinoff 1970). Generalized digital computer programs have been developed which use the finite difference method to simulate one-, two-, and three-dimensional nonsteady flow problems in heterogeneous aquifers under water table and artesian conditions (Prickett and Lonquist 1971 and Desai 1977). The finite difference method has been used to predict unsteady flow in gravity wells. Good agreement was found between computed results and laboratory test results obtained using a sand tank model (Desai 1977).

B-7. Finite Element Method.

a. Method of Solution. As previously mentioned in Chapter 4, the finite element method is conceptually a physical rather than a mathematical approximation. The flow region is subdivided into a number of elements and permeabilities are specified for each element. Boundary conditions are specified in terms of heads and flow rates and a system of equations is solved to compute gradients and velocities in each element (Desai and Abel 1972 and Desai 1977). Two- and three-dimensional finite element seepage computer programs for both confined and unconfined flow problems have been developed at WES. Steady-state and transient problems (that can be treated as a series of steady-state problems) can be solved (Tracy 1973a; Tracy 1973b; and Hall, Tracy, and Radhakrishnan 1975). An interactive graphics preprocessor is available to generate the finite element grid (Tracy 1977a). It is possible to compute the stream function and potential and plot contours of these values to obtain the flow net (Christian 1980 and Christian 1980). Details concerning the selection of spatial and time meshes, computer time required, convergence, and stability are available (Desai 1977). Also, an interactive graphics postprocessor is available to assist in the analyses of the finite element results (Tracy

1977b). A listing of finite element seepage computer programs used within the Corps is available (Edris and Vanadit-Ellis 1982).

b. Advantages. The finite element method is well suited to complex geometry, including sloping layers and pockets of materials of varying permeability. By varying the size of the elements, zones where seepage gradient or velocity is high can be accurately modeled.

c. Disadvantages. The finite element method is usually more costly than the finite difference method for simple problems (Rushton and Redshaw 1979).

d. Applications. The finite element method has been used in several cases to provide solutions to seepage problems.

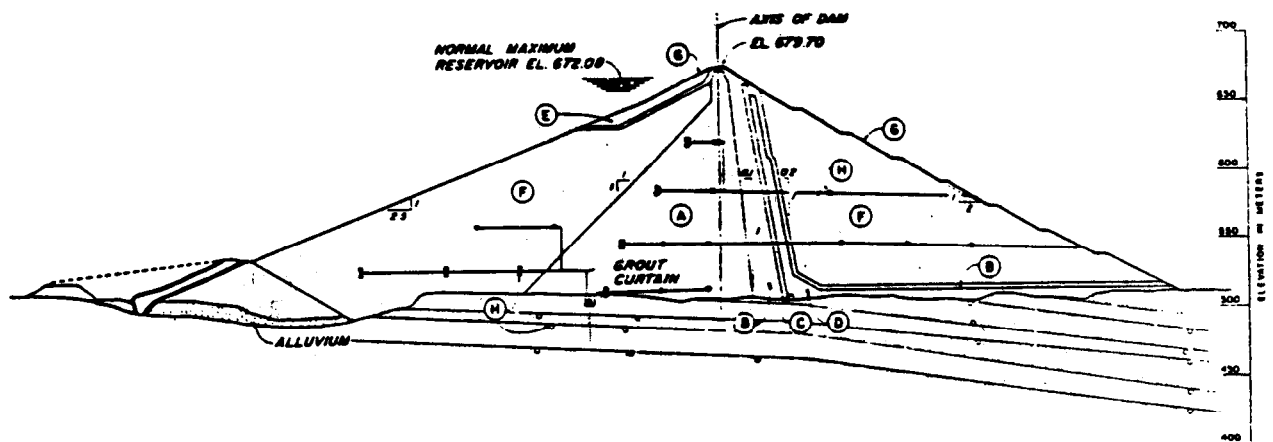
(1) WES studies. As discussed previously, the finite element method was used at WES to simulate seepage conditions in streambanks induced by sudden drawdown of the river level. This study included a viscous flow model, field observations, and application of the finite difference and finite element methods. The results of the study indicated that the finite element method provided satisfactory solutions for transient unconfined fluid flow in porous, anisotropic, and nonhomogeneous media (Desai 1970 and Desai 1973).

(2) Location of phreatic surface. The finite element method has been used to determine the location of the phreatic surface in earth dams (Isaacs 1979; Isaacs 1980; Wei and Shieh 1979; and Desai and Kuppusamy 1980). The finite element method was used to locate the phreatic surface within tailings pond embankments and to define the subsurface flow of water from the pond. Results predicted using the finite element model were confirmed with measurements in a laboratory model and in the field (Kealy and Busch 1971).

(3) W.A.C. Bennett Dam. The finite element method was used to assess the potential seepage flows and uplift pressures in the foundation rock for W.A.C. Bennett Dam in British Columbia, Canada (see figure B-21). The finite element analysis (see figure B-22) was carried out assuming the following conditions:

- (a) With an effective grout curtain.
- (b) Without an effective grout curtain.
- (c) With a drainage system.
- (d) Without a drainage system.
- (e) With various rock permeabilities.

The results of the finite element analysis, shown in figure B-23, indicate the greatest reduction in seepage flow and hydrostatic pressure could be accomplished by an effective grout curtain and downstream-drainage system (Taylor and Chow 1976).



- | | |
|---------------------------|------------------------|
| (A) Core. | (G) 2'-3' riprap. |
| (B) Transition. | (H) Piezometers : |
| (C) Filter. | ● Hydraulic type; |
| (D) Drain. | ▼ Vibrating wire type; |
| (E) Free draining gravel. | ○ Pneumatic type. |
| (F) Random shell. | |

Figure B-21. Cross section of W.A.C. Bennett Dam, British Columbia, Canada (courtesy of International Commission on Large Dams²⁶⁹)

(4) Corps of Engineers levees. The finite element method was used by the U. S. Army Engineer District, Rock Island, to study hydraulic sand fill levees along the Mississippi River (Schwartz 1976). Finite element and gradient plane⁽¹⁾ analyses were used in conjunction with data from a full scale test levee to establish the material properties of the sand levees and to determine the exit point of the free seepage surface, the quantity of through seepage, and the exit gradients along the free discharge face. A parameter study was performed and dimensionless design charts were developed.

(5) Reservoir loading conditions on zoned embankments. The use of the finite element method to study the effect of initial filling of the reservoir, steady seepage, and rapid drawdown of the reservoir on zoned embankments has been given (Eisenstein 1979).

(6) Bureau of Reclamation dams. The Bureau of Reclamation has utilized two- and three-dimensional finite element methods, electrical analogy, and mathematical methods to analyze seepage flow through a dam embankment and

(1) The gradient plane method is a graphical solution by means of the hodograph (see description by Casagrande 1937).

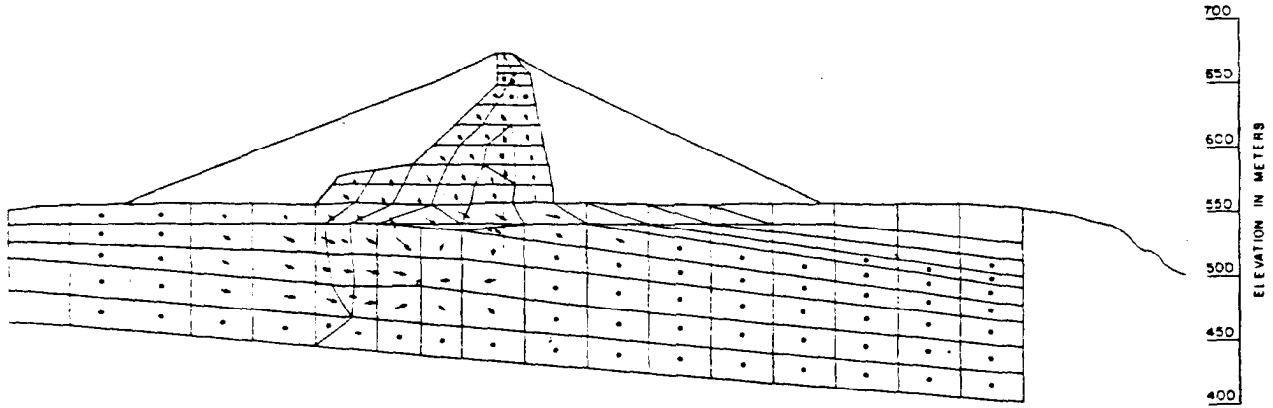
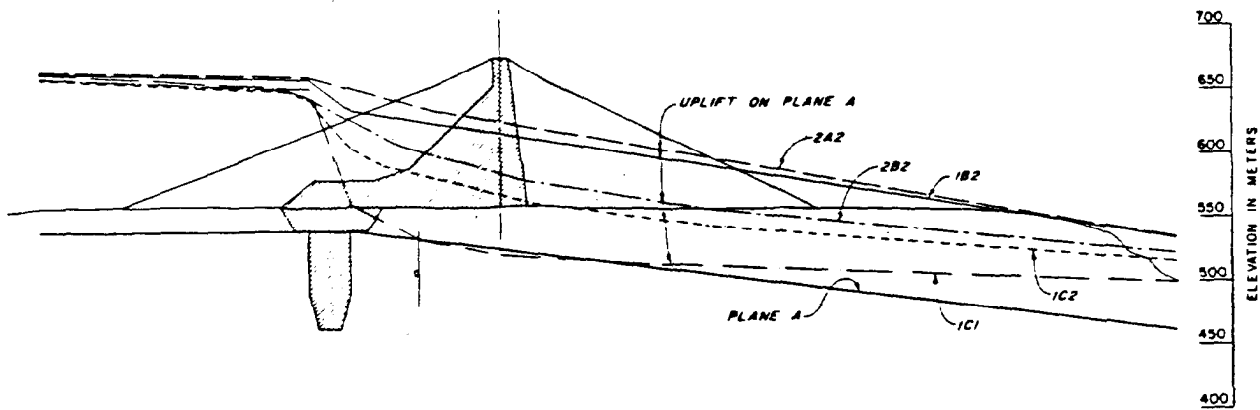


Figure B-22. Finite element study results (courtesy of International Commission on Large Dams²⁶⁹)



CASE	GROUT CURTAIN	DRAIN	K_H/K_V
1B2	YES	NO	10
1C1	YES	YES	1
1C2	YES	YES	10
2A2	NO	NO	10
2B2	NO	YES	10

Figure B-23. Uplift pressure under various conditions (courtesy of International Commission on Large Dams²⁶⁹)

foundation (Mantei and Harris 1979). Narrows Dam, Colorado, on the South Platte River, was analyzed for seepage at the feasibility stage. Because of a pervious foundation, the planners called for a positive vertical cutoff by constructing a slurry wall down to the underlying shale. However, near the right abutment the shale drops away to depths too great for economical slurry wall construction. A three-dimensional finite element model (see figure B-24) was used to determine the vertical exit gradients at the downstream toe of the dam. The finite element method was used to study the effect of a toe drain, partial depth slurry trench, partially and fully penetrating relief wells (see figure B-25). Calamus Dam, Nebraska, on the Calamus River, was also analyzed by the Bureau of Reclamation for seepage at the feasibility stage (Mantei and Harris 1979; Mantei, Esmiol, and Cobb 1980; Mantei and Cobb 1981; and Cobb 1984). Calamus Dam has a setting very similar to Narrows Dam in the sense that it is an earth dam on a pervious foundation. However, the underlying shale at Calamus Dam is at such a great depth that it cannot be used as the base for a cutoff wall as it was for Narrows Dam. Early thinking on the project involved the use of a slurry trench cutoff down to a pervious sandstone formation. A three-dimensional finite element model (see figure B-26) was used to determine the effects of an embankment toe drain, slurry trench under upstream blanket, and/or relief wells at the downstream toe of the dam on the seepage rates and hydraulic gradients in the dam foundation. Time and expense in operating the large three-dimensional finite element models made it necessary that priority be given to studying the various design alternatives using the best estimate of permeability for each foundation material rather than conducting sensitivity studies to establish the effect of varying the permeability (see paragraph B-1). The three-dimensional finite element models were five elements deep, with the bottom layer of elements representing the sandstone, the next layer sand and gravel, recent alluvium, interbedded fine sand, and dune sand. A detailed three-dimensional finite element model was made for the outlet works area that defined more of the design details, such as the filter blanket under the stilling basin and channel and water table elevation controls, to study the effectiveness of relief wells around the stilling basin.

(7) Corps of Engineer dams. The finite element method was used by the U. S. Army Engineer District, Huntington,⁽¹⁾ in a reanalysis of the underseepage at Bolivar Dam, Ohio, completed in 1938 on Sandy Creek (U. S. Army Engineer District, Huntington 1977a). A two-dimensional finite element model (see figure B-27) was used to determine the effects of an embankment toe drain, upstream impervious blanket, and proposed relief wells on seepage quantities, exit gradients, and uplift pressures. A sensitivity study was conducted using the two-dimensional finite element model to determine the influence of various pool and rock surface levels, the permeability ratio of foundation soils, the existence of a downstream gravel layer, and the effective source of seepage entry upon underseepage. Typical test results for one set of boundary conditions and permeability values are given in figure B-28. Additional applications of the two-dimensional finite element method to conduct sensitivity analysis to assess the effect of permeability anisotropy and various seepage control measures was given by Lefebvre and coworkers (Lefebvre, Part, and

(1) Work was performed by Soil Testing Services, Inc., Northbrook, Illinois.

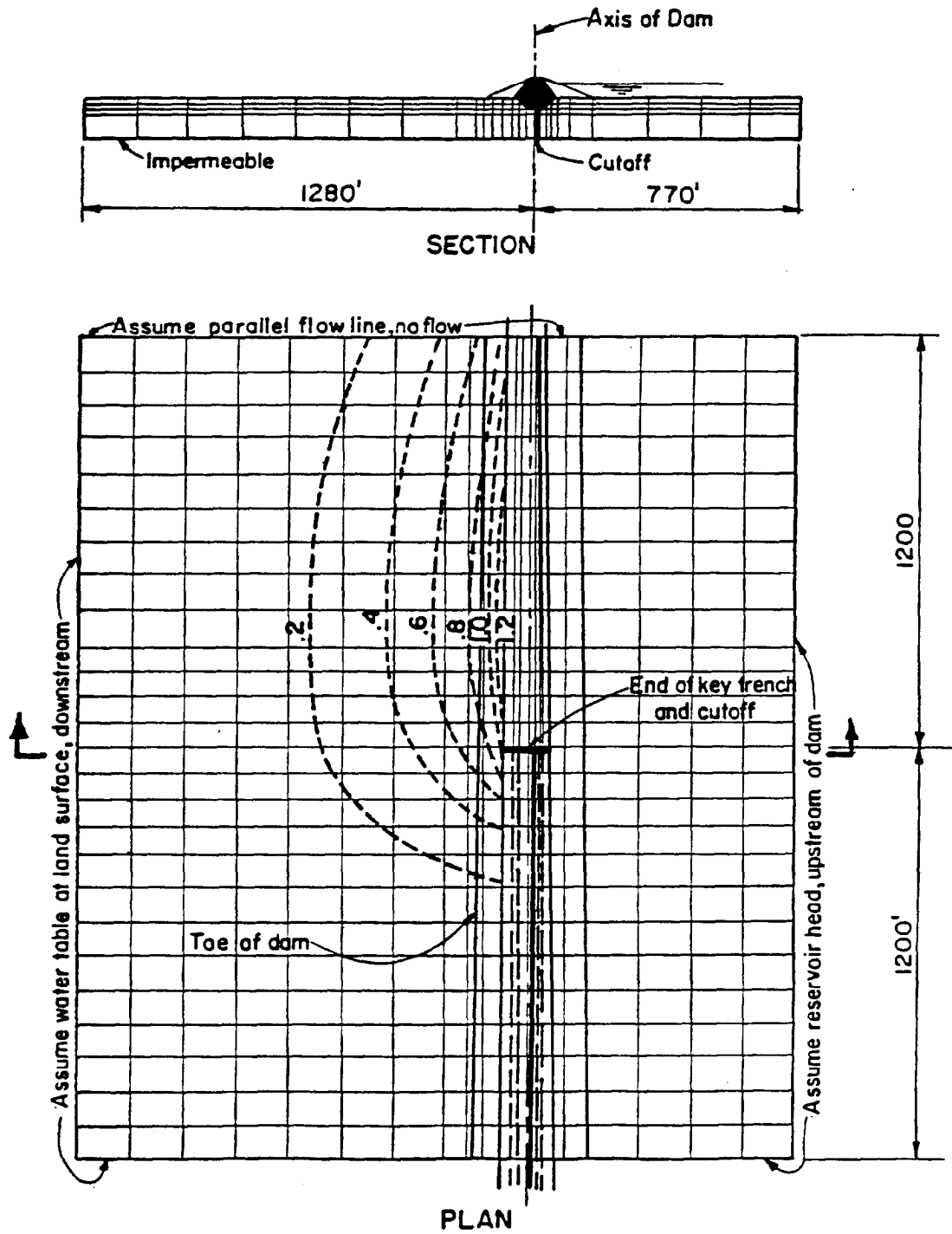
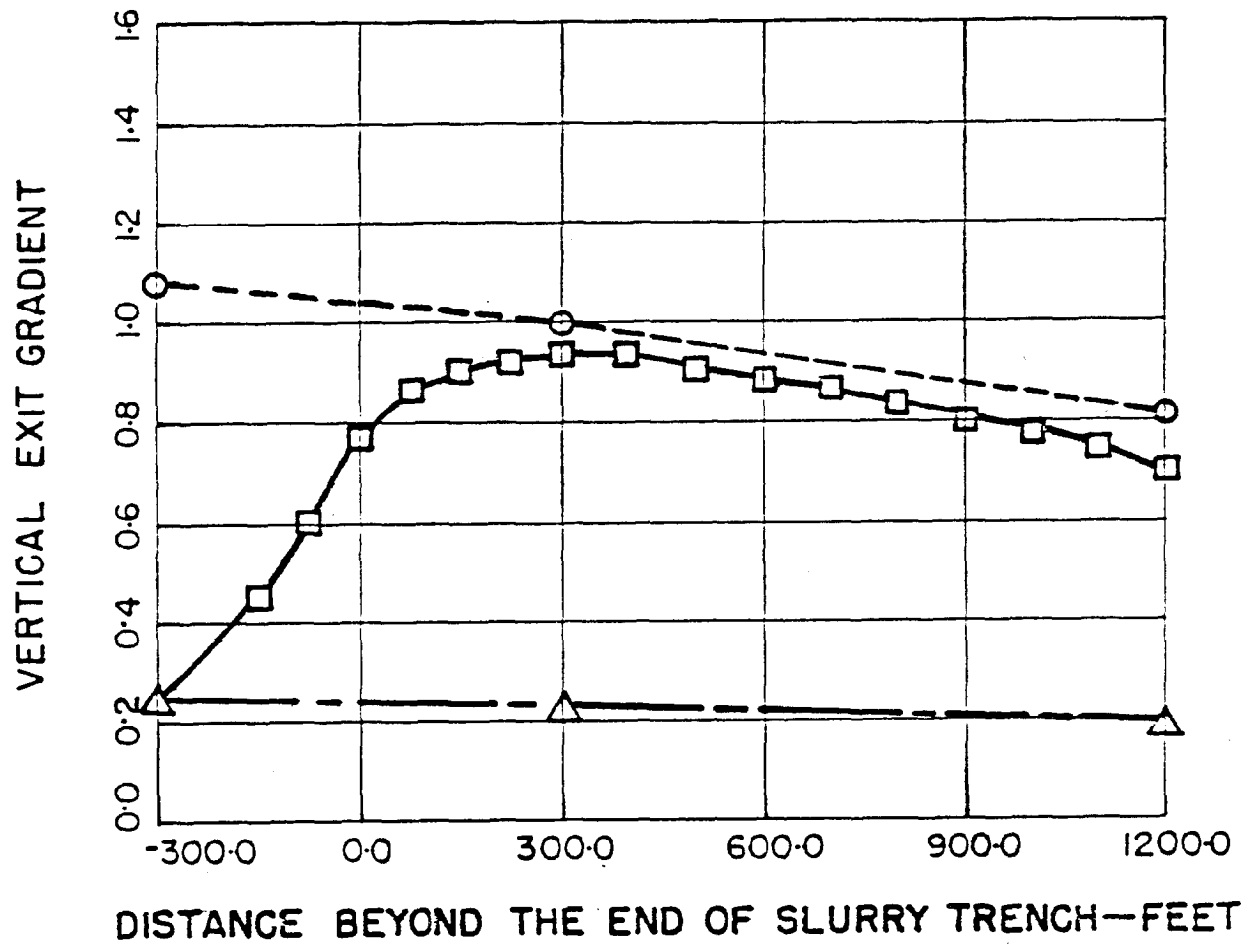


Figure B-24. Contours of exit gradient from three-dimensional finite element model study of Narrows Dam, Colorado (courtesy of American Society of Civil Engineers²¹⁷)

30 Sep 86



LEGEND

- 3-D MODEL WITHOUT RELIEF WELLS
- 2-D MODEL WITHOUT RELIEF WELLS
- △ QUASI 3-D MODEL WITH RELIEF WELLS AT 100' SPACING

Figure B-25. Vertical exit gradients from three-dimensional finite element model study of Narrows Dam, Colorado (courtesy of American Society of Civil Engineers²¹⁷)

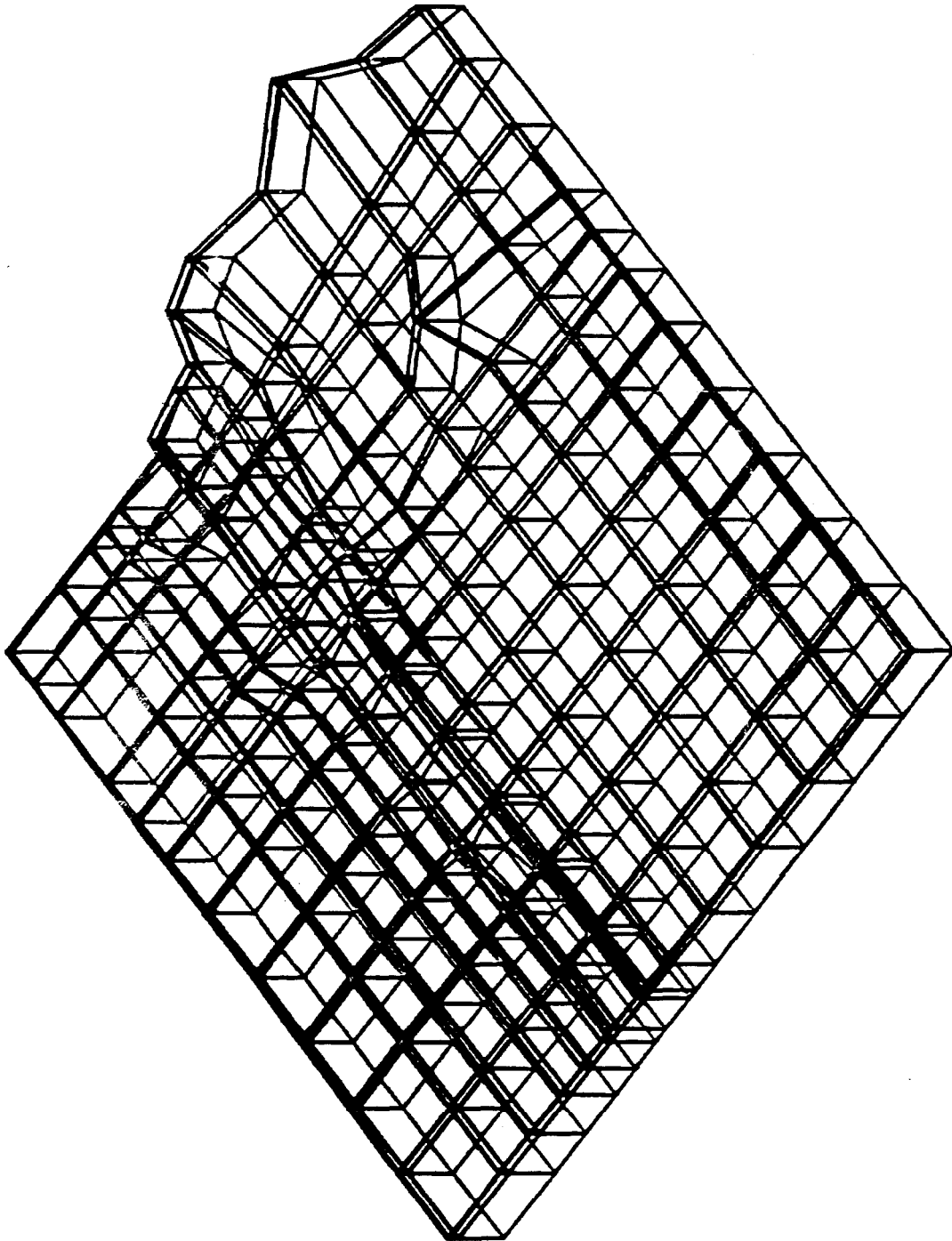


Figure B-26. Grid for three-dimensional finite element model study of Calamus Dam, Nebraska (courtesy of American Society of Civil Engineers²¹⁷)

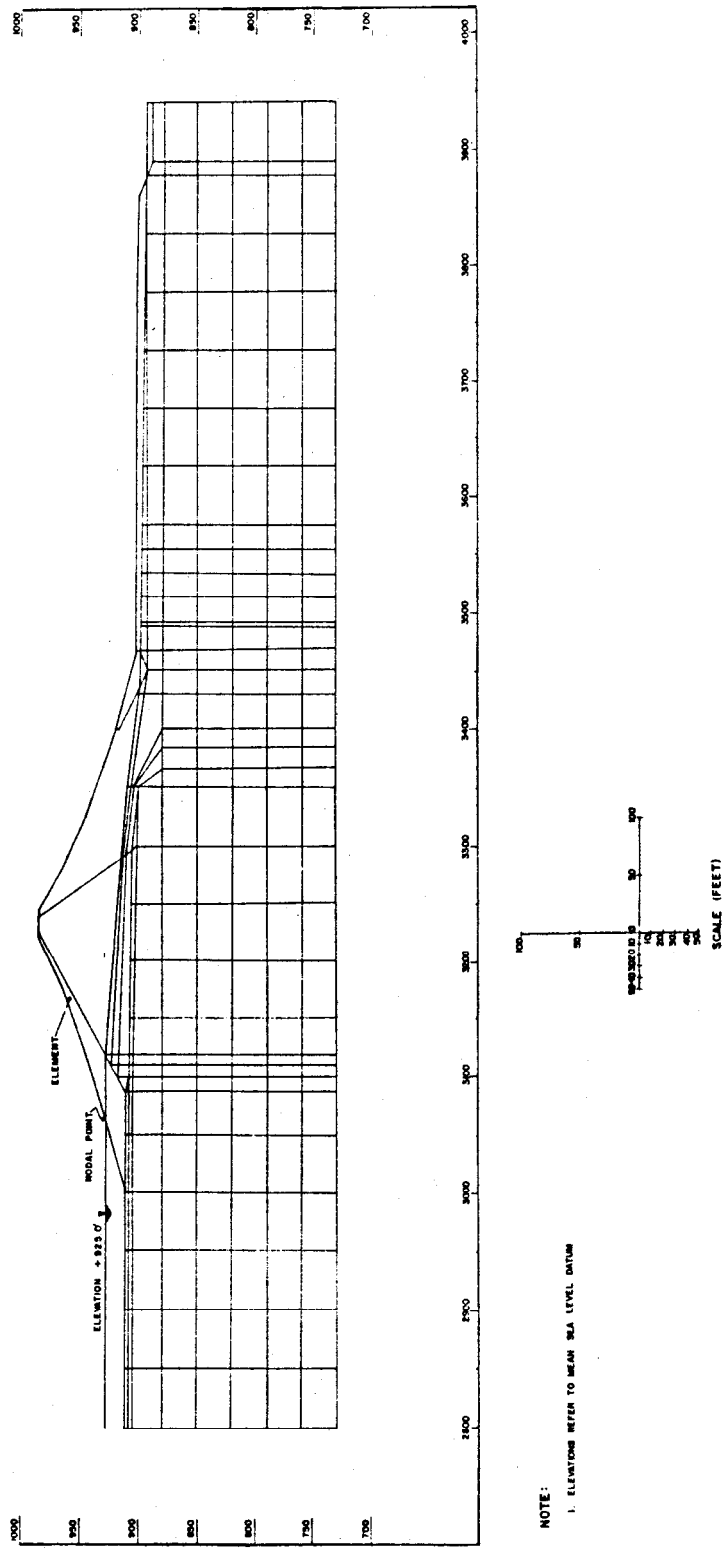


Figure B-27. Grid for two-dimensional finite element model study of Bolivar Dam, Ohio
(from U. S. Army Engineer District, Huntington⁸⁸)

30 Sep 86

Tournier 1981). The finite element method was used by the U. S. Army Engineer District, Huntington,⁽¹⁾ in a reanalysis of the underseepage at Mohawk Dam, Ohio, completed in 1937 on the Walhonding River (U. S. Army Engineer District, Huntington 1979b). A three-dimensional finite element model (see figure B-29) was used to study the cause of unusually high relief well flows. Typical test results for one set of boundary conditions are given in figure B-30.

⁽¹⁾ Work was performed by Soil Testing Services, Inc., Northbrook, Illinois.

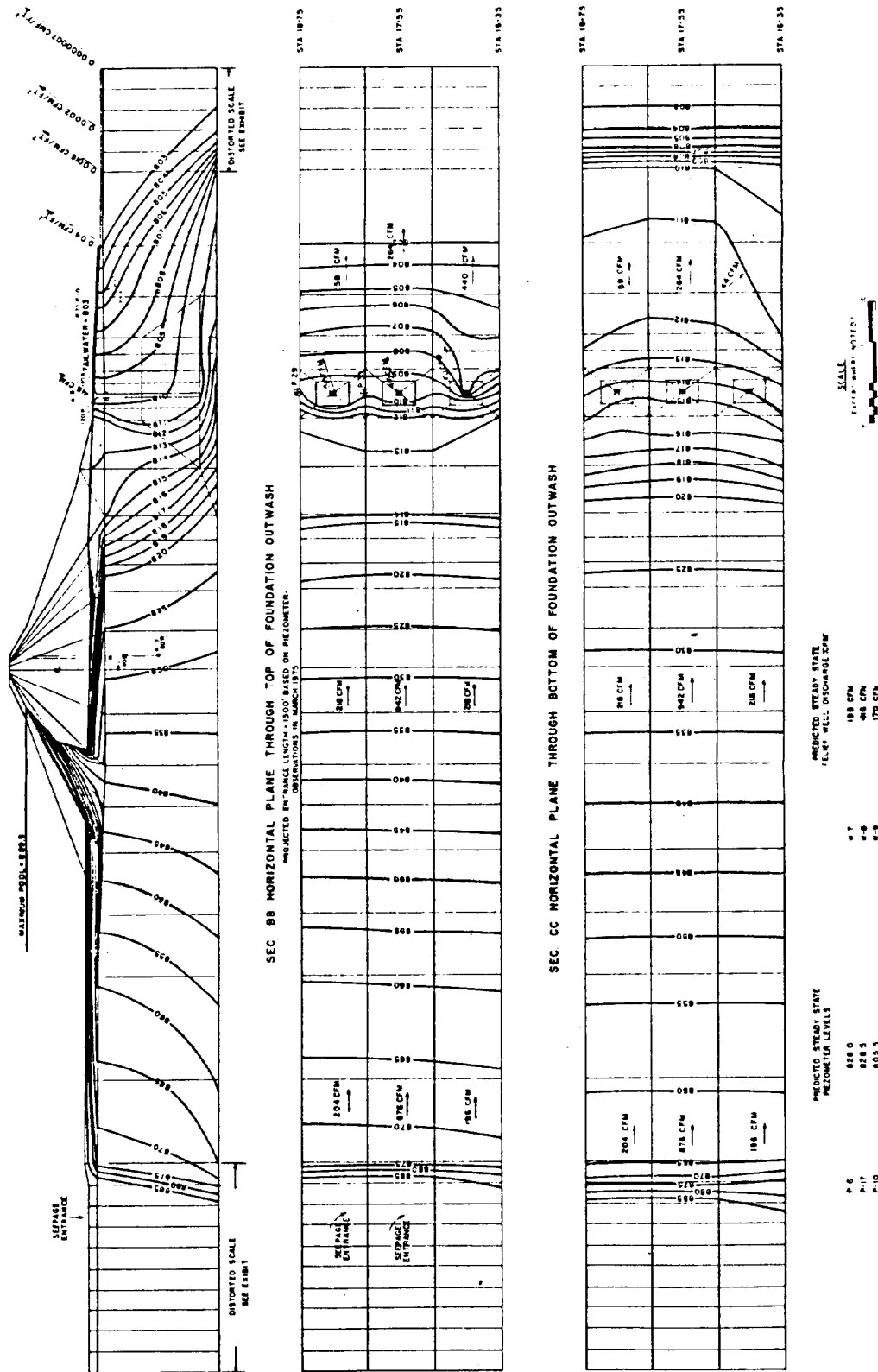


Figure B-30. Results from three-dimensional finite element model study of Mohawk Dam, Ohio
(from U. S. Army Engineer District, Huntington⁸⁹)